

Michael C Breadmore¹ 
 Wojciech Grochocki^{1,2}
 Umme Kalsoom^{1,3}
 Mónica N. Alves¹
 Sui Ching Phung¹
 Masoomeh Tehrani Rokh⁴
 Joan M. Cabot^{1,3}
 Alireza Ghiasvand^{1,5}
 Feng Li¹
 Aliaa I. Shallan^{6,7}
 Aemi S. Abdul Keyon^{8,10} 
 Ala A. Alhusban⁹
 Hong Heng See^{8,10} 
 Alain Wuethrich¹¹ 
 Mohamed Dawod¹²
 Joselito P Quirino¹

¹Australian Centre for Research on Separation Science, Chemistry, School of Natural Science, University of Tasmania, Hobart, Tasmania, Australia

Received September 12, 2018
 Revised October 15, 2018
 Accepted October 16, 2018

Review

Recent advances in enhancing the sensitivity of electrophoresis and electrochromatography in capillaries and microchips (2016–2018)

One of the most cited limitations of capillary and microchip electrophoresis is the poor sensitivity. This review continues to update this series of biannual reviews, first published in *Electrophoresis* in 2007, on developments in the field of online/in-line concentration methods in capillaries and microchips, covering the period July 2016–June 2018. It includes developments in the field of stacking, covering all methods from field-amplified sample stacking and large-volume sample stacking, through to isotachopheresis, dynamic pH junction, and sweeping. Attention is also given to online or in-line extraction methods that have been used for electrophoresis.

Keywords:

Extraction / Focusing / Preconcentration / Stacking / Sweeping
 DOI 10.1002/elps.201800384

1 Introduction

CE has always been regarded as having excellent mass detection limits, but poor detection limits when considered as concentration units. When compared to LC, it is typically 2 to 3 orders of magnitude worse particularly when using optical detection methods [1]. Approaches to improve the detection limits by exploiting various physical and chemical

phenomena have been developed over the past two decades and have been reviewed bi-annual by us [2–7], as well as reviews on this topic by others [8–28]. Over the last 2 years since the last update, there has again been considerable interest in this topic, with approximately 300 papers published in this time that discuss ‘stacking’ again indicating the importance of being able to perform sample treatment in a simple and automated manner.

This review will highlight developments within the field of online concentration for electrophoresis, in both capillaries and microchips. The review is not comprehensive, and instead discusses works that are of significance to the field published between July 2016 and June 2018. Classifications that have been used previously will be kept here and the material has been assembled in the same categories: concentration approaches based on electrophoretic phenomena, will be broadly discussed as ‘stacking’, while those involving partitioning onto or into a distinct phase, will be considered as ‘extraction’. This review will discuss approaches within the context of these two broad areas with the critical requirement that they are integrated in some manner, preferably “in-line” (performed within the capillary) or “online” (performed in a completely integrated and automated manner). For those who would like a more practical focus, Breadmore and Sanger-Van De Griend propose a decision tree to help select the right method for the right application [29].

Correspondence: Professor Michael Breadmore, Australian Centre for Research on Separation Science, School of Chemistry, University of Tasmania, GPO Box 252–75, Hobart, Tasmania 7001, Australia.

Fax: +61-3-6226-2858

E-mail: mcb@utas.edu.au

Abbreviations: μ CGE, micro-capillary gel electrophoresis; μ PAD, microfluidic paper based analytical device; AFMC, analyte focusing by micelle collapse; BMAA, β -N-methylamino-L-alanine; CD, cyclodextrin; DLLME, dispersive liquid–liquid microextraction; EDL, electric double layer; EKS, Electrokinetic supercharging; FASS, field-amplified sample stacking; FISH, fluorescence in situ hybridization; FLM, free liquid membrane; HDI, hydrodynamic injection; ICP, ion concentration polarization; LE, leading electrolyte; LVF, large-volume focusing; LVSS, large-volume sample stacking; LVSEP, LVSS using EOF pump; MCDS, micelle to cyclodextrin stacking; MCE, microchip capillary electrophoresis; M-ITP, multiple ITP; NMI, nano-microchannel interface; REPSM, reversed electrode polarity stacking mode; SEF, sensitivity enhancement factor; SLM, supported liquid membrane; TE, terminating/trailing electrolyte; tITP, transient ITP

Color online: See article online to view Figs. 1, 3, 4, 6–10, and 13 in color.

2 Stacking

2.1 Field-strength induced changes in velocity

2.1.1 Field-amplified sample stacking and field-amplified sample injection

Field-amplified sample stacking (FASS) is perhaps the oldest and most well-known online sample preconcentration technique [30, 31]. In FASS, sample prepared in a low conductivity diluent is injected hydrodynamically into the capillary filled with higher conductivity BGE. Application of high voltage across the capillary results in higher electric field strength in sample zone than in BGE. Consequently, analytes in sample zone move rapidly until they reach sample/BGE interface or 'stacking boundary' where their velocities are slowed down abruptly and analytes' focusing occurs. The conductivity ratio between sample diluent and BGE determines the sensitivity enhancement factor (SEF) that can be obtained by FASS. Theoretically, the conductivity ratio 10, 100, or 1000 would result in SEF 10, 100, or 1000, respectively. However, in practice typical SEFs are around 10–20. This is because of mismatch in local electroosmotic velocities in sample zone and BGE, which causes peak broadening if the injected sample plug is larger than 5% of the total capillary volume. Another restriction of FASS is that only low conductivity samples can be concentrated and thus, additional sample pretreatment steps such as sample dilution or desalting are required.

Kerrin et al. [32] reported a quantitative determination on the neurotoxin β -N-methylamino-L-alanine (BMAA) in different types of shellfish by FASS-CZE coupled with MS/MS. A strong cation exchange SPE was used as a sample clean-up procedure to obtain field-amplified conditions. The sample extracts were reconstituted in 2 mM HCl and injected hydrodynamically for 240 s at 50 mbar which corresponded to injection volume of 200 nL or 10% of the total capillary volume. Despite the fact that sample injection volume was two times bigger than typical sample injection volume in FASS, a good resolution between BMAA and other isomeric amino acids was obtained. The LOD for BMAA was 0.8 ng/mL which corresponded to 16 ng/g dry mass sample. This was similar to LOD of BMAA reported for the HILIC–DMS–MS/MS assay.

If sample ions are injected electrokinetically, rather than hydrodynamically, then this is known as field-amplified sample injection (FASI) [30, 31]. When the high voltage is applied, charged analytes enter the capillary by their own electrophoretic mobility as well as by EOF and focus at the stacking boundary, which is found at the inlet tip of the capillary between low conductivity sample diluent in a sample vial and BGE inside the capillary. To avoid analyte's loss as well as to improve reproducibility of the sample injection, a short plug of low conductivity solvent is usually injected into the capillary prior to electrokinetic injection [33–36]. FASI allows to improve the sensitivity up to 1000 \times . However, only cationic or anionic analytes can be concentrated in a single analysis.

Zhang and Meagher [37] reported three orders of magnitude sensitivity improvement by using FASI in SDS-CGE of adeno-associated virus (AAV) capsid proteins. The LOD of 0.2 ng/mL was achieved with conventional UV detection. This was comparable with LOD values obtained by using traditional SDS-CGE with LIF detection or silver stained SDS-PAGE. However, the new method did not require time- and labor-consuming labeling procedure and only 25 ng of total AAV capsid proteins were needed in purity analysis of AAV therapeutic products. The developed method can be adopted for size-based analysis of other types of proteins, especially, when protein quantity or concentration is not sufficient for regular SDS-CGE or SDS-PAGE assay.

Zeid et al. [38] used FASI in a microchip-EKC method for determination of gabapentin and pregabalin in pharmaceutical and biological matrices. Both analytes were labeled with 4-fluoro-7-nitro-2,1,3 benzoxadiazole followed by separation in poly(methyl methacrylate) microchip equipped with a light emitting diode-induced fluorescence(LED-IF) detector. FASI allowed to improve the sensitivity 17- and 14-fold for gabapentin and pregabalin, respectively, compared to traditional pinched injection. The LOD was < 3 ng/mL for both analytes. The developed method was applied for the analysis of both drugs in pharmaceutical and biological (plasma and urine) samples after simple dilution with purified water and acetonitrile, respectively, followed by derivatization procedure.

FASS and FASI are usually the first choice among all stacking techniques due to their simplicity and high compatibility with different CE modes such as CZE [39–50], EKC [51–54], CGE [37], CEC [55, 56] as well as microchip electrophoresis [38, 57]. An uncomplicated buffer system used in FASS and FASI allows to utilize a whole range of detectors including UV [37, 39, 41–45, 47–51, 53–56], LED-IF [38], LIF [57], C4D [46], and amperometric [52]. The sample matrix effect is reduced or eliminated since the sample clean-up is necessary to lower the conductivity of the sample and thus, FASS and FASI can be used in analysis of biological [38, 41–45, 47, 48, 56, 57], pharmaceutical [37, 38], environmental [49, 52], food [46, 50, 51, 54, 55], industrial [39], and forensic samples [53]. In addition, combination of FASS and FASI with other stacking techniques is popularly used in multi-stacking approaches which will be discussed further in this review.

2.1.2 Large-volume sample stacking

Large-volume sample stacking (LVSS) was developed to overcome the peak broadening issues as observed with FASS and improve the concentration efficiency. LVSS allows the hydrodynamic injection of a large volume of low conductivity sample, up to 95% of the capillary volume is filled with sample, which is later stacked prior to the separation of the analytes. It is most easily achieved by polarity switching where the voltage is applied to direct EOF toward the inlet of the capillary for matrix removal from the injection end and to stack analytes on

the sample/BGE boundary, which slowly moves back toward the inlet too. When most of the sample matrix is removed, indicated by the current reaching 90–95% of the BGE current, the polarity is switched to allow separation of the stacked analytes. Fundamental to this approach is that the electrophoretic mobilities of the analytes must be opposite to that of the EOF. LVSS with polarity switching has been broadly used for highly sensitive analysis of a wide variety of analytes including antibiotics (e.g., chlortetracycline, doxycycline, oxytetracycline, and tetracycline) in milk and environmental water samples [58, 59]; camptothecin alkaloids (e.g., Camptothecin, 9-methoxycamptothecin, 9-aminocamptothecin, 10-hydroxycamptothecin, and 7-ethyl-10-hydroxycamptothecin), a potential antitumor drug isolated from the bark and fruit of a Chinese tree [60]; active ingredients (rutin, hyperoside, and chlorogenic acid) in herbal medicine [61]; and food-borne pathogen, *Salmonella typhimurium* in water samples. Although LVSS with polarity switching is very popular, meticulous current monitoring makes automation of LVSS using commercial CE system a challenging task.

LVSS using EOF pump (LVSEP) is a very simple and efficient stacking technique that does not require polarity switching. In LVSEP, the EOF that is smaller and opposite to the electrophoretic mobility of the analytes is used to pump the sample matrix out of the capillary. LVSEP has been used for sensitive and efficient determination of nitrate and nitrite in canned fish samples [62]; D- and L- isomers of aspartate and glutamate with enrichment factor of 480 [63]; antimicrobial agent, pentamidine in rat plasma [64]; ammonia, amines (including cyclohexylamine, ethanolamine, morpholine, hydrazine, dimethylamine, and triethanolamine) and their degradation products, e.g., methylamine, ethylamine, and diethanolamine in steam water [65]; and DNA fragments [66]. Multistep pressure assisted LVSEP, in which injection of large sample volumes and pressure assisted electroosmotic pumping of the sample matrix out of the capillary was performed in repeated cycles to improve the sensitivity (enhancement factors up to 170) of amyloid β (A β) peptides, biomarkers for Alzheimer's disease diagnosis, in cerebrospinal fluid [67].

LVSEP in combination with FASI has also been employed to significantly improve the sensitivity. For example, Kitagawa et al. [68] observed 4520-fold sensitivity enhancement for fluorescein when LVSEP was used in combination with FASI, 33-times higher sensitivity in comparison to when only LVSEP was used for stacking.

In addition to LVSEP, the sample matrix removal without polarity switching has also been achieved by utilizing the difference in pH of the sample solution and BGE. For example, Wu et al. performed LVSS by injecting sample solution of cationic tetracycline at pH 4.6, which became negatively charged while the sample matrix was being removed by BGE (pH 11.0) on the application of negative voltage. Although some loss of cationic tetracycline was observed, it reduced with an increase in BGE pH with an enhancement factor of 35–44 obtained at pH 11 [69].

2.1.3 Isotachophoretic stacking

Among all preconcentration methods in electrophoresis, ITP is one of the most robust and powerful because it can concentrate trace components in a high concentration of matrix ions. In ITP, the sample is concentrated between the leading electrolyte (LE) and the terminating/trailing electrolyte (TE). The difference in mobility between the leader (higher mobility) as compared to terminator (lower mobility) creates a non-uniform electric field upon application of voltage such that ions with a mobility between leader and terminator ions stack in behind the LE but in front of the terminator, in descending order based on their mobilities. The length of each zone depends on the concentration of each ion—when the concentration is insufficient to reach the steady-state concentration defined by the Kohlrausch regulating function then the ion is concentrated as a sharp 'peak' between adjacent ITP zones. ITP induces concentration and separation at the same time, but can also be coupled in a transient manner to CZE and other modes of electrophoresis, both of which are discussed below.

2.1.3.1 ITP

One of the most widely used techniques for the identification and quantification of bacteria is fluorescence in situ hybridization (FISH). FISH often targets 16S and 23S ribosomal RNA (rRNA) within intact bacterial cells with routinely obtained detection limits of 10^3 to 10^4 cells/mL [70]. Although this is a rapid technique comparing to plate counting, it takes 2 h before detection to fix and stain the bacterial cells. Phung et al. [71] developed a counter-pressure-assisted ITP method in combination with a sieving matrix and ionic spacer to examine ITP-accelerated hybridization for in-line FISH staining of intact bacterial cells. In the first stage, bacterial cells and FISH probe are concentrated and focused in a small volume at the ITP interface allowing cell hybridization with the probe. In the second stage, the bacterial cells are separated from the free probe by means of a sieving matrix. This method offered comparable LOD with the CE analysis of a sample processed using an offline FISH protocol (6.0×10^4 cells/mL), but reduced the analysis time significantly from 2.5 h to 30 min and can be done fully automated within the CE instrument [71].

Moreno-Gordaliza et al. [72] established an ITP method to resolve 18 lipoprotein peaks from serum and plasma. This was achieved using a mixture of 24 spacers that was carefully selected based on the predictive software PeakMaster. This method was statistically comparable to NMR analysis of human plasma samples in terms of group-clustering and lipoprotein species correlation and was applied to the lipoprotein profiling of an LDL receptor knock-out mice model fed with a normal diet and a western-type diet. [72].

Mai et al. [73] used multiple ITP (M-ITP) based on the repetition of successive cycles of hydrodynamic injection (HDI) and ITP to improve detection sensitivity (Fig. 1). Sample is

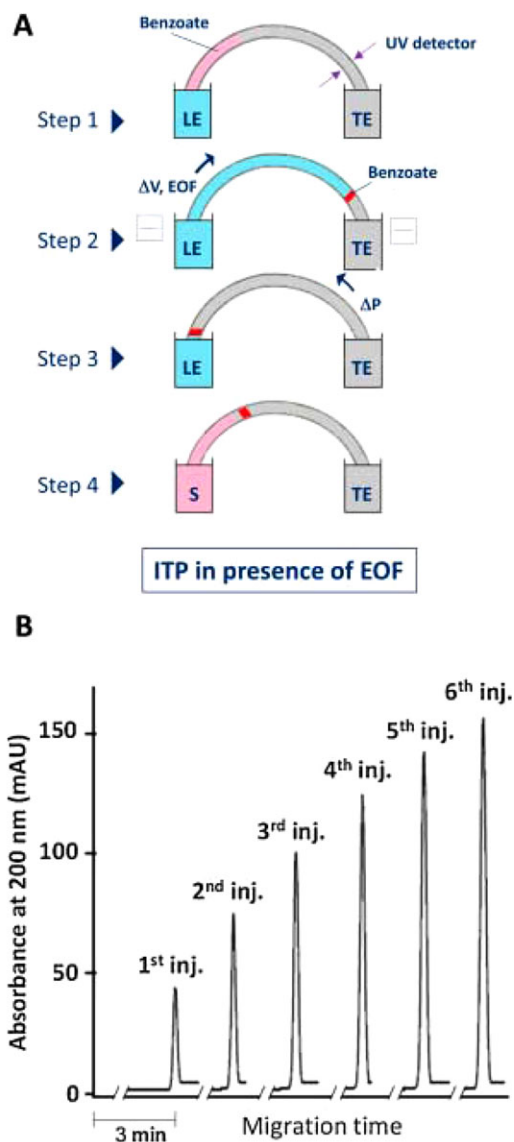


Figure 1. (A) Demonstration of the M-ITP process under alkaline conditions with the presence of a strong EOF. Sample (S): benzoate; TE co-anion: borate; LE co-anion: acetate; (B) M-ITP of benzoate (100 μM) prepared in LE under alkaline conditions with the presence of elevated EOF. LE solution: 50 mM NH_4OH /10 mM CH_3COOH (pH 9.9); TE solution: 96.6 mM boric acid/40 mM NaOH (pH 9.2). The M-ITP was performed with LE and TE at the inlet and outlet ends of the capillary, respectively. The injected sample plug length in each ITP cycle was 30 cm. Constant current mode $I = 20 \mu\text{A}$. Reproduced from [73] with permission.

initially injected and separated by ITP but stopped before it exits the capillary and pushed by pressure to the inlet. A second HDI is performed and ITP performed again, with the process repeated until a sufficiently high enrichment has been achieved. Imidazole was used as model for cationic analyte and benzoate as anionic analyte to validate this approach. Each cycle took 8.5 and 3 min to complete for imidazole and benzoate, respectively. The peak area of imidazole and benzoate increased linearly with the injection number over

nine and six ITP cycles with a coefficient of determination r^2 of 0.9998 and 0.9997, respectively. However, the linearity of peak height over injections was good only for the first six cycles (r^2 of 0.9972) for imidazole and four cycles (r^2 of 0.9972) for benzoate. The M-ITP method was applied to amyloid peptide A β 1–40, which is a well-established biomarker for early diagnosis of Alzheimer's disease [73].

On-chip ITP systems are an excellent alternative to capillaries as it offers much higher flexibility in setup, although shows lower sensitivity and efficiency. The use of microchip ITP has been mainly focused on low molecular mass analytes and DNA separations as most of the standard nucleic acids isolation protocols are based on difficult and laborious extractions. The Santiago group's introduced ITP as an alternative means to purify and isolate DNA over a decade ago, and this has been shown to be simple and powerful approach for DNA analysis [74, 75]. Eid et al. demonstrated an ITP-Recombinant polymerase amplification (RPA) assay for detection of inactivated *Listeria monocytogenes* from whole blood samples [76]. ITP was used to purify the lysed bacterial DNA from whole blood in a single ITP channel. The purified DNA in the extraction reservoir is then transferred to standard recombinant polymerase amplification master mixture for 25 min thermal cyclers at 40°C. The LOD of the genomic DNA was 16.7 fg/ μL (5×10^3 cells/mL). The method allows detection of chemically inactivated *L. monocytogenes* cells in whole blood at 2×10^4 cells per mL. Later, Eid et al. then reported the use of ITP with ionic spacer and sieving matrix to preconcentrate and separate the preconcentrated NA based on their size. A rapid prototyped laser-cut PMMA microfluidic device with modifiable channel dimension allows larger sample volume (10 μL) to be used, and have an in-line extraction reservoir for manual collections of the size-fractionated NA [77]. A mixture of single stranded DNA and/or RNA mixture with different nucleotide length was used as a proof of concept with the first fractions consisting of small NAs (96% DNA, 87% RNA) and the second fractions consisting of both small and large RNAs. The whole process took 10 min without the need of NA labels or microscopy. However this approach is unable to generate fractions with a sharp cut-off as the electrophoretic mobility dependent separation method results in significant dispersion when the NA mobilities are closer to the spacer or TE.

Kooten et al. [78] reported a large-volume focusing (LVF)-chip design whereby at initial, a larger sample volume can be used (50 μL) and preconcentrated into a concentrated zone with a volume of 500 pL using ITP. The LVF chip has a wide region tapering down to 100-fold narrower channel together with a geometrical feature designed to reduce dispersion arising from the non-uniform entry of the ITP interface into the narrow region. This design allows the dimensions of the chip to be scaled up for larger sample volume without the loss of focusing. When the LVF chip was compared with the standard glass chip using a pre-labeled DNA, a 310 000-fold increase in peak concentration was obtained allowing direct detection of 10 fM DNA. The LVF chip was used for DNA hybridization between molecular beacon and DNA probe using ITP with

reported LoD of 1 pM at 10 s reaction time. For bacterial cell detection, the LVF chip could detect cells stained with SYTO 9 at 100 cfu/mL.

Sydes et al. [79] presented an on chip intersection potential measurement targeted to control the electromigration and electroosmosis in multichannel networks in ITP using histidine and arginine. The authors showed that the ITP step of His and Arg were observed when the measured potential reached 3.5 kV, with a repeatability within 1.4% ($n = 3$). Hradski et al. [80] used simulations to study the factors that affect ITP quantitation in a microchip using conductivity detection and compared with experimental validation. They showed robust ITP analysis of acetate, yet a small run-to-run fluctuation in the driving current was considered as the main factor limiting the reproducibility of quantitation. The use of suitable internal standard significantly improved the precision by six to eight times. The calibration curve of acetate in two different microchip and equipment with recovery data from 98 to 101% was shown.

Marczak et al. [81] reported a gel-membrane microchip with probe functionalized nanoparticles for quantification of short nucleic acid using depletion ITP. Their method relies on an ion-selective membrane to pre-concentrate the probe-functionalized nanoparticles and the target molecules using ion enrichment and achieve rapid target hybridization. The electric field is then reversed to form a depletion region. When the depletion zone reaches the nanoparticles, a selective aggregation of the dimer particles is induced while driving the monomer particles down toward the channel via ITP. Gel is used in the microchannel as an EOF suppressor. The concentration of the DNA target was measured using optical quantification of the plasmon resonance band of the dimer particles. The total analysis time reported was <20 min with LOD of 10 pM (69-bp ssDNA) and is highly selective against non-targets with a three decade linear range for quantification with selectivity and signal intensity are maintained in heterogeneous mixtures. Marczak et al. [82] later improved the selectivity by increasing the voltage during depletion step to selectively dehybridize the nonspecifically adsorbed molecules as the high electrical shear force can dehybridize the non-targets and/or mismatched molecules in seconds. This method was highly selective against two mismatch non-target (35 bp sequences) with both having no detectable signal.

Loessberg-Zahl et al. [83] reported a proof of concept on a quasi-stationary ITP method for concentration or separation in a nanochannel induced by charge inversion. A simple analytical model was used to locate the front position of the charge inversion mediated-ITP concentration boundary. They exploit the charge inversion and ITP in the nanofluidic system to create an almost stationary sample-focusing zone. $\text{Ru}(\text{bpy})_3\text{Cl}_2$ was used in this study to induce the charge inversion and also allow visualization due to its natural fluorescence property. One of the advantages of this method is that it has minimum dispersion and eliminates extra experimental components or surface coating. In addition, the natural fluorescence of $\text{Ru}(\text{bpy})_3\text{Cl}_2$ allows continuous, real-time monitoring of the front location.

Rosenfield and Bercovici [84] optimized a novel microfluidic paper based analytical device (μPAD) by utilizing the native high EOF in the nitrocellulose to achieve a stationary ITP focusing for direct detection of the 16s rRNA of *Escherichia coli* Morpholino-based probe. From the experimental data, the authors showed the total signal of probe-target hybrids versus time for initial concentration of 5, 10, and 100 pM of the DNA target. From the total accumulated data (three replicates), the time required for certain detection of each concentration is 10, 5, and 3 mins for 5, 10, and 100 pM, respectively. In the final stage of the study, the authors performed a multiplex on the μPAD consisting of 12 assays operated in parallel using 1 μM fluorescein in a 24-well plate. The authors reported that all of the 12 ITP interfaces were formed and remained stationary during the analysis.

Kalman et al. [85] reported a single step kinetic assay (homogeneous free solution) whereby free sequence specific probes are continuously separated from the probe-target during focusing, allowing the monitoring of the dissociation kinetics. A non-focusing probe is used as a continuous injection ITP to give rise to a unique accumulation-dissociation dynamic to achieve a highly specific detection in presence of high concentration of mismatch. The author started with an analytical model studying followed by experimental for validation. One of the advantages of this assay is that it enables gain signal owing to ITP focusing while dissociating any nonspecific hybrids. The standard CCD-based optical system shows an LOD of 100 pm, allowing demonstration of 1:1000 specificity for 4/25 bps sequences and 1:10 specificity for 20/25 bp sequences.

2.1.3.2 tITP

When ITP is used in the transient ITP (tITP) mode, an initial ITP zone is created, and then after steady state has been reached, the ITP zone is dissipated and the ITP-stacked components are separated by CZE or another mode of electrophoresis.

An innovative tITP-CZE method with a system induced terminator was demonstrated by Hattori et al. [86] for determination of aniline and pyridine. One of the particularities of the described method is the use of water instead of TE. The BGE was composed of 100 mM acetic acid and 50 mM sodium hydroxide (pH 4.6). The sample was injected after the capillary was filled with BGE. Sodium, aniline, and pyridine migrated to the cathode and acetate and chloride to the anode by electrophoresis, which resulted in a sample-vacancy zone being created. The concentration of acetate increased in the sample vacancy zone since it continuously migrated from the BGE at the front end of the sample zone. Simultaneously, hydronium was generated from water in the vacancy zone thus, the cationic analytes were sandwiched and concentrated between sodium (leading ion) and hydronium (terminating ion) by tITP. A water vial was subsequently set at the sample-inlet side and 25 kV were applied for the separation of aniline and pyridine (Fig. 2). The respective LOD of aniline and pyridine were 10 and 42 g/L that corresponds to an improvement of

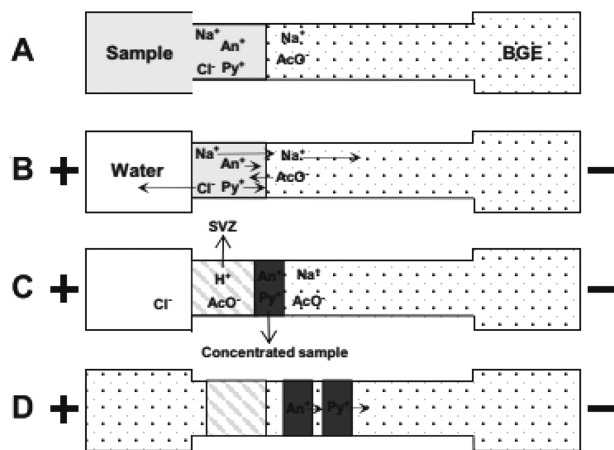


Figure 2. Schematic of the tITP-CZE method with a system induced terminator. (A) the capillary is filled with BGE and the sample is injected, (B) Na^+ , An^+ , and Py^+ migrates electrophoretically to the cathode and AcO^- and Cl^- to the anode electrophoresis, (C) a sample vacancy zone (SVZ) is formed and analytes are concentrated by tITP, and (D) separation of the analytes by CZE. Reproduced from [86] with permission.

17 and 14 times compared to the conventional CZE method. This method was applied to sewage samples [86].

The determination of fluoride (F^-) in seawater is important to monitor and regulate the concentration of this anion in agreement with wastewater standards in Japan. For this purpose, absorptiometry and ion chromatography have been used, however they require several steps prior analysis. Fukushi et al. [87] developed a tITP-CZE method with indirect UV detection for the determination of F^- in seawater. The optimum conditions for the BGE were 5 mM 2,6-pyridinedicarboxylic acid adjusted to pH 3.5 containing 0.03% (w/v) hydroxypropylmethylcellulose. The LOD for F^- was 0.024 mg/L. This method was simple, not requiring sample pretreatment aside from filtration and tenfold dilution [87].

Crevillén et al. developed an on-chip tITP method for α -lactalbumin and β -lactoglobulin. Using the optimized electrolytes, separation of both fluorescently labeled proteins was achieved in less than 4 min with peak resolution of 1.5 and limit of detections were 55 and 380 nM, for α -lactalbumin and β -lactoglobulin, respectively. This sensitivity was adequate for some food allergenicity studies [88].

2.2 Chemically induced changes in velocity

2.2.1 Dynamic pH junction

This methodology concentrates target analytes via a change in pH between the BGE and sample. When an analyte's ionization state changes due to a variation in pH, its electrophoretic mobility is altered and can cause concentration and focusing. This change in ionization depends on the pK_a values of analytes in the sample. For instance, for a monoprotic acidic

compound with pK_a of 6, at pH 4, it will be 1% ionized but at pH = 8, it will change to 99%. This was first applied to CE by Aebersold and Morrison [89] in 1990 and termed dynamic pH junction in 2000 by Britz-McKibbin et al. [90], but it is also known as a moving neutralization boundary [91] and is a subcategory of moving reaction boundaries [92].

Dynamic pH junction is a simple online sample preconcentration method well-suited for amphiprotic analytes, especially peptides and proteins. In just 2 years, there has been up to seven publications on bottom-up and top-down proteomics using CZE-ESI-MS. Dovichi's group [93] has recently shown in a mini review that dynamic pH junction-based CE-ESI-MS system has been widely applied for proteomic analysis, including *E. coli* proteome and phosphoproteome from human cell line. Zhang et al. [94] used this technique to further improve the preconcentration performance from an online SPE. They prepared the sample in 1 M acetic acid, eluted using 0.2 M ammonium bicarbonate (pH 8), and finally perform the separation using the change in pH from these two solutions. They applied this method for bottom-up proteomics, identifying 145 protein groups and 365 peptides in 5.5 ng *E. coli* digest. Better peptide separation is required for bottom-up proteomics for further improving the proteome coverage. Using dynamic pH junction, Chen et al. [95] developed an approach for 500 nL loading capacity and 140 min separation window and high peak capacity (~380) for large-scale proteome analysis of mouse brain digests. The BGE of CZE was 5% (v/v) acetic acid and samples were adjusted to pH 8.0 using 10 mM NH_4HCO_3 . Next year, same authors [96] established a strong cation exchange HPLC separation followed by CZE-MS/MS for deep bottom-up proteomics. Up to 60 HPLC fractions were dissolved in few microliters of ammonium bicarbonate (pH 8.0) and injected for separation using BGE of 5% (v/v) acetic acid at pH 2.4. They could identify around 8200 protein groups and 65 000 unique peptides from a mouse brain proteome digest. Total analysis time for one sample was 70 h. Zhao et al. [97] explored its potential for intact protein characterization, top-down proteomics. Five hundred eighty proteoforms and 180 protein groups were identified from the 23 fractions of a previous offline HPLC separation, claiming to be the largest top-down proteome dataset based on this technique reported to date. Next year, Lubeckyj et al. [98] carried out a comprehensive study on dynamic pH junction for direct analysis of top-down proteomics. A comparison with FASS demonstrated that dynamic pH junction could efficiently concentrate protein molecules with even 500 nL of sample injection volume (25% capillary length, Fig. 3) and increasing the number of theoretical plates by 3.5-fold (myoglobin). They identified with a single-shot of 1 μL from *E. coli* proteome approximately 600 proteoforms and 200 proteins. Alternatively, McCool et al. [99] presented an orthogonal multidimensional separation platform that couples SEC and RPLC based protein prefractionation to CZE-MS/MS for deep top-down proteomics of *E. coli*. Again, dynamic pH junction allowed preconcentration from 500 nL sample loading, sample was adjusted to pH 8 with 50 mM NH_4HCO_3 (pH 8.0) and BGE was 10% acetic acid. This platform

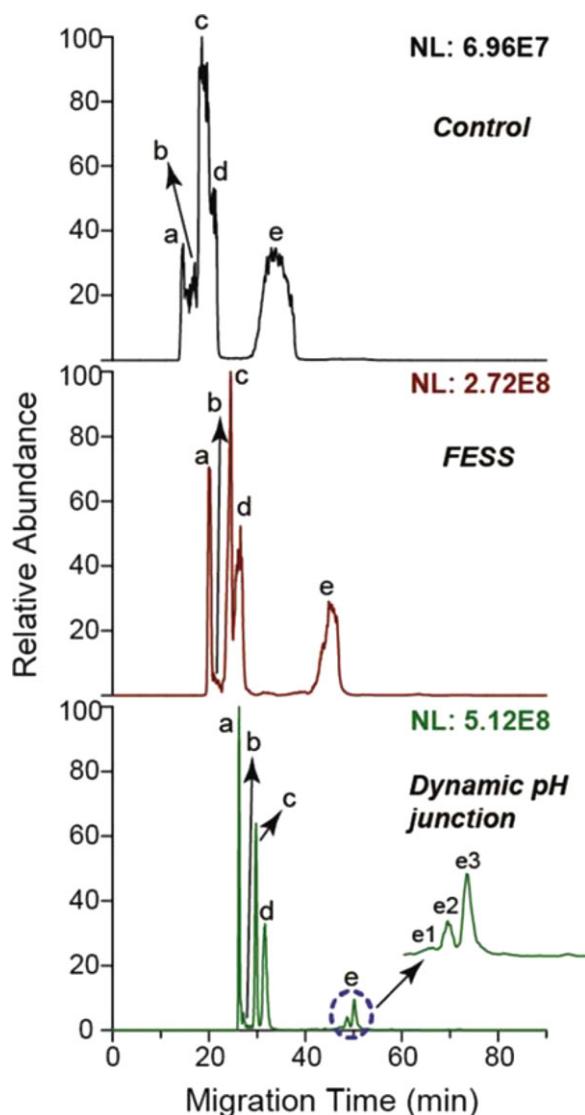


Figure 3. Extracted ion electropherograms of the mixture of standard proteins from CZE-MS under the three different conditions. The sample injection volume was 500 nL for each condition. The proteins labeled in the electropherograms are (a) lysozyme, (b) cyto.c, (c) myoglobin, (d) CA, and (e) β -casein. The four proteins (lysozyme, cyto.c, myoglobin, and CA) were extracted with m/z 1590.33, 765.33, 808.20, and 880.55, respectively. The standard protein mixture was dissolved in 50 mM NH_4HCO_3 (pH 8.0) analyzed by the dynamic pH junction-based CZE-MS. Reproduced from [98] with permission.

generated high peak capacity (~ 4000) leading to the identification of 5700 proteoforms from the *E. coli* proteome.

Yasuno and Fukushi [100] developed an improved dynamic pH junction to determine sub-micromolar phenol in seawater. They used borate buffer at pH 9.8 (close to the pK_a of phenol) and hexadimethrine bromide to reverse EOF. A 30 mM solution of *n*-hexanoate was injected after the sample, probably to maintain high pH values after sample plug during separations. That allowed the phenol to concentrate

in the boundary between the fatty acids and sample (around pH 11 as predicted by computer simulation) and be separated from the impurities. They reached LODs of 5.9 ppb at 190 nm.

2.2.2 Association with pseudo-stationary phases

The separation of cationic, anionic, and especially neutral analytes is accomplished in EKC through their interaction with a pseudostationary phase or pseudophase (e.g., micelles) [101, 102]. This interaction can also be used for sample concentration through sweeping, the accumulation of the analytes at the front of the pseudophase [7, 13, 103, 104], and release of micelle-bound analytes and accumulation at a stacking boundary by analyte focusing by micelle collapse (AFMC) [105], micelle to solvent stacking (MSS) [106, 107], and more recently by micelle to cyclodextrin stacking (MCDS) [108].

2.2.2.1 Sweeping

In sweeping, analytes are focused as narrow bands using a pseudophase such as micelles [109]. The efficiency is mainly dependent upon the interaction of the analytes with the pseudophase. This method is usually coupled with offline cleanup methods such as liquid–liquid extraction (LLE) [110], SPE [111], dispersive micro-SPE [112], solid-phase microextraction [19], and dispersive liquid–liquid microextraction (DLLME) [113–115], to remove matrix interferences.

The stationary and moving boundaries in sweeping processes for online focusing in EKC were considered as the accelerating or decelerating planes and modeled for better understanding of the sweeping mechanism [116]. This strategy was used to measure triazine herbicide in honey, tomato, and environmental water samples after hollow fiber liquid–liquid–liquid microextraction pretreatment [117]. Sweeping-MEKC was used also for quantification of organophosphorus pesticides (chlorfenvinphos, parathion, quinalphos, fenitrothion, azinphos-ethyl, parathion-methyl, fensulfothion, methidathion, and paraoxon) in medicinal plants after sample preparation by ultrasound-assisted DLLME [118]. Sweeping-MEKC was also coupled with MS/MS and used for the therapeutic monitoring of benzimidazoles in animal urine [111]. The sensitivity enhancement factors (SEFs) were found to be over the range 50–181 for albendazole, albendazole sulfone, albendazole sulfoxide, carbendazim, benomyl, fenbendazole, fenbendazole sulfone, fenbendazole sulfoxide, mebendazole amino, mebendazole, oxbendazole, thiabendazole, and hydroxymebendazole.

Sweeping is typically performed from a single boundary. Sanuki et al. [119] have demonstrated double sweeping, in which sample components were swept from different sides of the sample by using cationic micelles on one side of the sample, and anionic micelles on the other. The micelles migration continued until the two moving fronts met at the ‘collision point’ where micelles stopped to move due to mixing of cationic and anionic micelles (see Fig. 4).

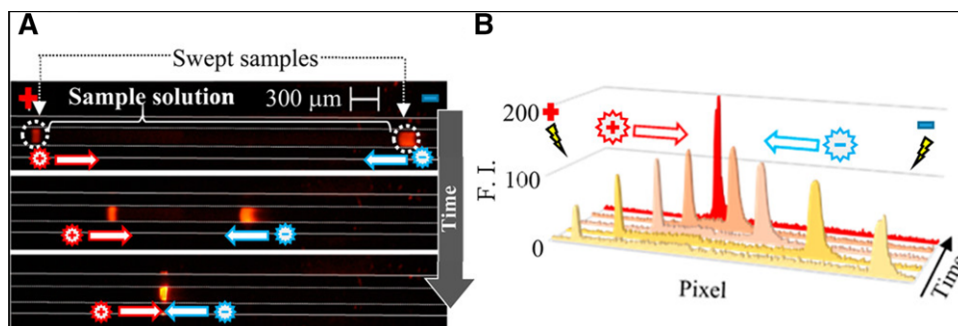


Figure 4. Sample preconcentration by double sweeping. (A) Fluorescence images obtained by digital microscope at 13, 27, and 42 s after applying voltage. (B) Fluorescence intensity profiles extracted from fluorescence images. Reprinted with permission from [119]. Copyright (2018) American Chemical Society.

Therefore, analytes were focused into very narrow bands close to the collision point. Double sweeping was shown to provide significantly more effective preconcentration than conventional sweeping, especially in the case of the simultaneous preconcentration of weakly, moderately, and highly hydrophobic products, which are difficult to concentrate simultaneously by conventional sweeping.

Conductivity detection has become a popular alternative to absorbance detection especially in modern chip-based devices, however, the use of high concentrations of charged pseudophases compromises this form of detection. To overcome this limitation, sweeping can be performed with a neutral pseudophase. Boublik et al. [120] studied such systems theoretically using combination of computer simulations and experimental data and a model provided for a reliable prediction of the enrichment factor. It was revealed that the conductivity signal was remarkably affected by slowing down the analyte, therefore, the cumulative signal enhancement can easily outweigh amplification caused solely by the sweeping phenomenon. In addition, possible formation of unexpected system peaks was revealed computationally and demonstrated experimentally, which may compromise separation and detection. Limits of detection were improved by 10.8–76.8.

2.2.2.2 AFMC, MSS, and MCDS

In contrast to sweeping, in which molecules are concentrated by association with the pseudophase, AFMC, MSS, and MCDS achieve concentration by disrupting the association of transported analytes by destroying or collapsing the micelles. Since their introduction a decade ago, this approach has evolved as a powerful approach to online concentration.

To improve the performance of micelle release in AFMC, a short volume of pure water was injected prior to the sample in MEEKC for measurement of phthalate esters, as neutral analytes, in pediatric pharmaceuticals. Here, the pure water plug (acting as the micellar dilution zone) enhanced micelles collapse when they migrate into the dilution zone [121]. The presence of micelles in sample matrix provided charge for neutral analytes to move and also improves their solubility (see Fig. 5). Under the optimal experimental conditions SEFs for benzyl butyl phthalate, dibutyl phthalate, diethylhexyl

phthalate, and diisodecyl phthalate were 86, 90, 200, and 58, respectively.

MSS relies on the reversal in effective electrophoretic mobility of charged analytes at the stacking at the boundary between organic solvent-rich and micellar solution zone and thus the micelles should have opposite charge to the analyte [106]. This was recently implemented in a microchip using Rhodamine B as a model cationic analyte and anionic micelles added to the sample and the channel filled with 50 mM phosphoric acid in 70% methanol [122]. Injection of the stacked analyte was performed by reversal of the polarity with the sample solution and separation media at the anodic and cathodic reservoirs, respectively, of the straight channel. A sensitive MSS method was introduced for online separation and concentration drugs of abuse and their metabolites in human urine. In this way, four amphetamines, cocaine, cocaethylene, heroin, morphine, 6-monoacetylmorphine, and 4-methylmethcathinone were stacked and analyzed through an MSS–CZE method [123]. The developed MSS–CZE method provided 39–55-fold enhancement in sensitivity. MSS has been also used successfully for sample cleanup in a new research [124]. SDS is used generally for protein solubilization in proteomic studies, while its presence interferes with mass spectrometric analysis of proteins. This study presented an electrokinetic SDS removal procedure prior to ESI–MS analysis.

In MCDS, the reversal of effective electrophoretic mobility is caused by cyclodextrins (CDs), which form inclusion complexes with long chain ionic surfactants and cause collapse of the micelles [108]. Schematic representation of MCDS mechanism of anionic analytes using cationic micelles and neutral CDs in CZE is shown in Fig. 6. The fused silica capillary coated with a cationic polyelectrolyte is conditioned and filled with a basic background solution (BGE), which also ionizes the analytes. Then, a long plug of sample containing micelles (i.e., CTAB) and analytes in the BGE is injected followed by injection of neutral CD in the BGE. The conductivity of BGE, CD, and sample solutions should be similar to avoid stacking or destacking by field enhancement or reduction. The direction of EOF and micelle migration are opposite. Analytes are bound to the positively charged micelles and migrate to the MCDS boundary between the CD and sample (see Fig. 6B) where the micelles collapsed due

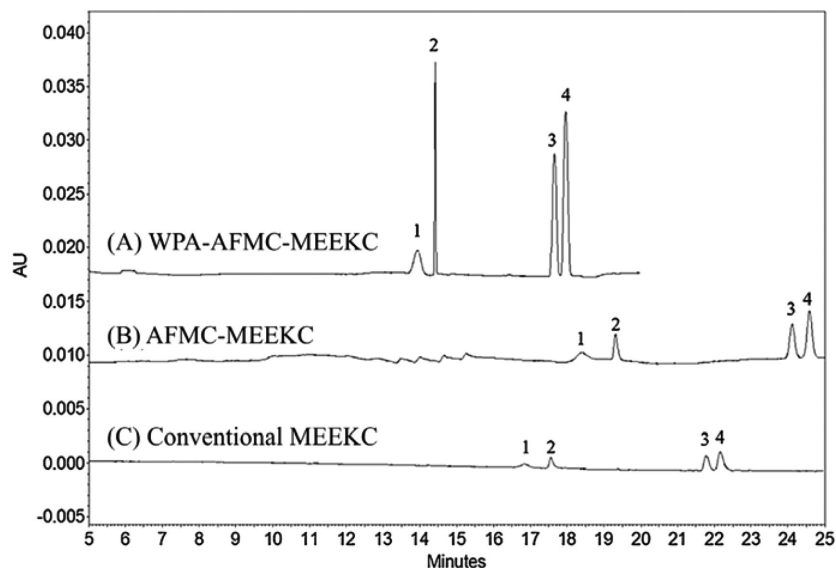


Figure 5. Comparison of the electropherograms obtained by A) water plug assisted (WPA) AFMC-MEEKC method, B) AFMC method alone, and C) the conventional MEEKC procedure. The analytes (1–4) are phthalate esters with concentrations of 1–50 $\mu\text{g/mL}$. Reproduced from [121] with permission.

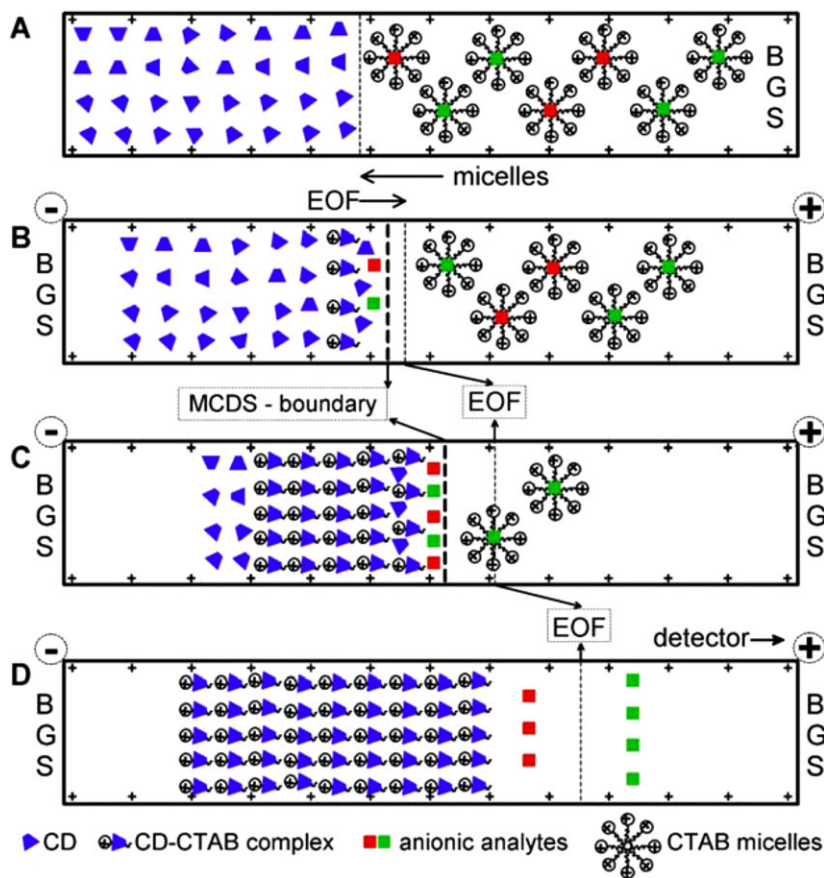


Figure 6. Schematic presentation of MCDS mechanism for anionic analytes using cationic CTAB micelles and neutral CDs in CZE. (A) The starting situation, conditioning, and injection. (B and C) The stacking process, and (D) the separation from the detector. Reprinted with permission from [108]. Copyright (2017) American Chemical Society.

to the formation of inclusion complexes between CD and CTAB. The analytes are released (see Fig. 6C) and can be concentrated. The stacking ends when all the micelles migrated through the “dynamic” boundary, and this is followed by separation by CZE (see Fig. 6D). For cations, the separation media was an acidic buffer and the pseudophase was from SDS,

which has opposite charge compared to the analytes. SEFs of 236–445 and 101–76 for the cationic and anionic analytes, respectively, were achieved and relative standard deviations (RSD%) were found to be 3.8–5.7%. The proposed stacking method was also carried out for direct analysis of peptides in trypsin digested bovine serum.

2.3 Physically induced changes in velocity

Electric field strength gradients for online preconcentration can be easily generated near nano-microchannel interfaces (NMIs). Preferential electrokinetic transport of counter-ions through the nanochannels in NMIs is observed when the diameter of the nanochannel approaches the electric double layer (EDL) thickness resulting in a complete or partial EDL overlap. When an electric field is applied across the NMI, counter-ions participate in the EDL and carry the charge through the nanochannel while co-ions are excluded. For a negatively charged surface, enrichment and depletion zones will evolve on the cathodic and anodic sides of the NMI, respectively. A concentration gradient is created inside these zones resulting in an electric field strength gradient where ions of interest can be concentrated in the enrichment zone or on the border of the depletion zone. This phenomenon is called ion concentration polarization (ICP) and exhibits a unique voltage–current curve consisting of three regions; ohmic, limiting, and over-limiting behavior. The key to achieve high enrichment factors is to balance the forces acting on the concentrated sample plug, namely; the ICP, EOF, and electrophoretic forces. Many factors affect this balance including the ionic strength, pH, surface charge density, and temperature. The main disadvantage of the ICP-based preconcentration techniques is that enrichment factors quickly

deteriorates for higher ionic strength samples, which is the case for most biological samples.

2.3.1 Nafion™ membrane

Nafion is by far and away the most frequently used material for ICP due to its versatility and the number of ways in which it can be included into a device. Chen et al. integrated a nanoscale Nafion membrane into PDMS microchannel for ICP preconcentration, separation, and collection. Two different channel configurations, straight and convergent microchannels, were compared in terms of the preconcentration factor using FITC labeled BSA as a model analyte. The device with convergent channel showed a higher preconcentration factor of 50, while only 40 was achieved for the straight channel device. By combining with a magnetically actuated valve, it was possible to separate and collect preconcentrated FITC-BSA and Tetramethylrhodamine mixtures [125].

Kim et al. [126] presented a micro/nanofluidic device for simultaneous desalting and sample preconcentration. The device consisted of an anodic multiple-branched microchannel and a cathodic single-branched microchannel as shown in Fig. 7; both anodic and cathodic microchannels were fabricated with PDMS, and were connected to each other via a Nafion membrane. Using this device, most of the salt ions (65%) were transported through the Nafion membrane to the

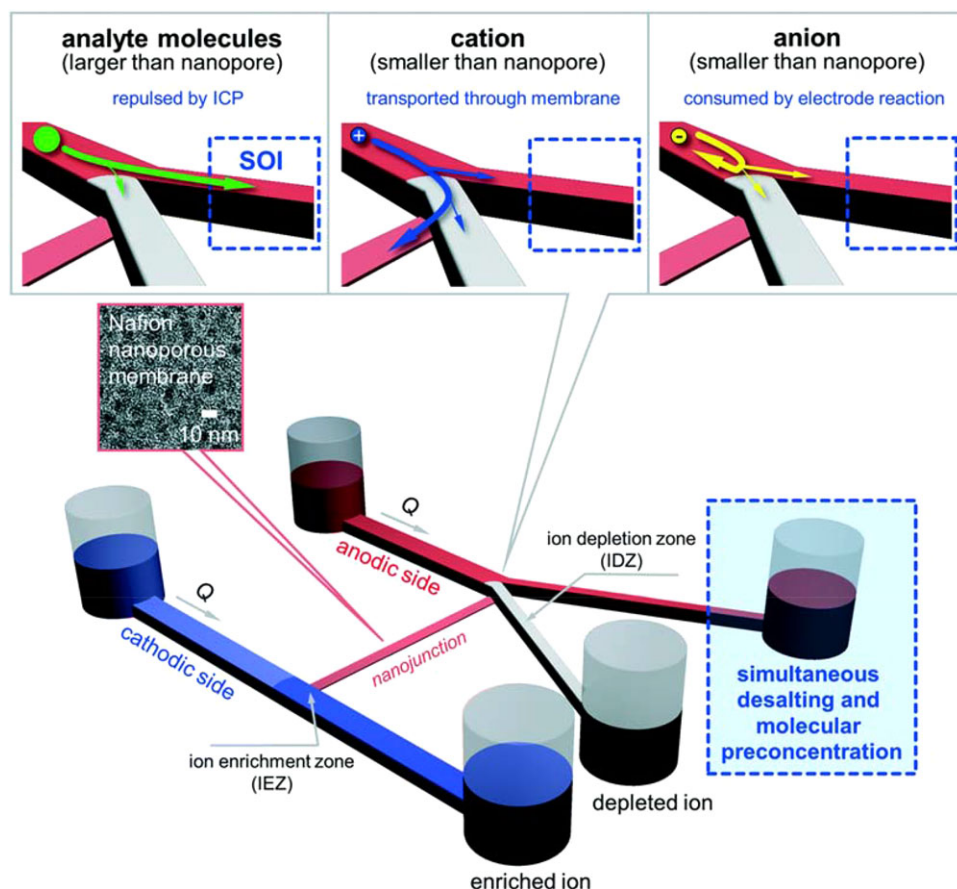


Figure 7. Schematic diagram of bifurcated system for ICP operation. Repulsion by ICP and cation flux through the nanojunction caused the rearrangement of concentration distributions at the entrance and the exit of the nanojunction. Nafion was utilized as a nanojunction, which has a pore size of less than 10 nm (see TEM image). The simultaneous desalting and molecular preconcentration process would be expected at the region outside the ion depletion zone (red), which was set to be the SOI (stream of interest). Reproduced from [126] with permission from the Royal Society of Chemistry.

cathodic side, the remaining anions were consumed by electrode reactions for electro-neutrality requirements, while the analytes were repelled by the ICP due to the larger size than the nanopores and preconcentrated.

Nafion™ can be easily integrated into paper-fluidic devices as a liquid, and dried, however it can block the channel and decrease the fluidic flow leading to poor enrichments. To solve this problem, Chou et al. [127] introduced an origami folding paper device design where Nafion was pipetted to cover one layer within the reservoir and leaving 10% hydrophilic margin to aid the flow through the device (Fig. 8). A convergent channel at an angle of 17° was employed. By applying an external voltage of 40 V, a 1 nM FITC-BSA in 10 mM Tris buffer was enriched by 100-fold after 135 s.

A simple device design composed of a 10-mm straight paper strip cut using an electronic craft cutter was reported for enrichment of two gene fragments, namely; muc1 (945 bp) a breast cancer marker and lamp-2 (185 bp) a marker for

Danon disease [128]. The NMI was created by pipetting Nafion (0.5 μL) in the middle of the paper strip. Both ends of the device were immersed in reservoirs filled with 10 mM KCl and connected to Ag/AgCl electrodes. The fluorescently labeled gene fragments in 10 mM KCl were enriched by applying 50 V then reversal of the electric field polarity after 10 s. The concentrated sample plug in the enrichment zone was further enriched on the depletion boundary when the polarity was reversed. The enrichment factors were 20-fold for muc1 and 60-fold for lamp-2 after 120 s.

Liu et al. [129] directly pipetted Nafion™ onto one end of the convergent paper fluidic channel before inclosing it with parafilm. Laminating parafilm on both sides of the paper strip increased the durability of the device and minimized evaporation. As the parafilm is embedded in the paper, the channel thickness is less than the original 180 μm, which means that the sample plug is more confined than with normal paper. A convergent channel design was employed to further increase the enrichment factors. The device was pre-wetted with 10 mM CaCl₂ before loading a 5 μL aliquot of the sample. A 5 μM solution of FITC in ionized water was enriched by 100-fold after 250 s using an applied voltage of 50 V.

An efficient approach to achieve high enhancement factors was decreasing the channel thickness. Yeh et al. [130] demonstrated that double sided wax printing followed by heating at controlled temperature reduced the channels depth available for separation from 180 μm to 50 μm. The design was a single 20 × 1.3 mm straight channel and Nafion was pipetted at a point half-way along the channel length to form the NMI. As a result of the reduced EOF and the confinement of the sample plug, the device showed remarkably higher enrichment factor as compared to other ICP-based μPADs. A solution of 10 nM FITC-BSA in 10 mM Tris buffer was enriched by 835-fold within 30 min using an applied voltage of 200 V.

Although forming the NMI by pipetting Nafion directly on the paper is easy, there is no control over the shape of the formed membrane and more importantly the flow through the paper fibers can be blocked unless a hydrophilic zone is included in the device design. A more accurate way to create the NMI is to pattern Nafion on adhesive tape then assemble the different layers together. Laminating cation and anion selective NMIs to μPADs was reported for concentrating fluorescein by 10-fold and Rhodamine 6G by 50-fold after 800 s, respectively [131]. Reversal of the EOF using CTAB was essential when using the anion selective membrane.

In a different approach to incorporating Nafion™, Han et al. [132] showed that enrichment factors can be greatly increased by sandwiching the paper channel between two laminated Nafion membranes. A 15 μM FITC-BSA in 100 mM NaCl was enriched by 310-fold using an applied voltage of 200 V. Tween 20 (0.01%) was added to the BGE to minimize protein adsorption. To balance the forces acting on the concentrated plug, they introduced two absorbent pads. Another approach is to laminate two Nafion membranes on both sides of the sample reservoir, but only fivefold enrichment factor

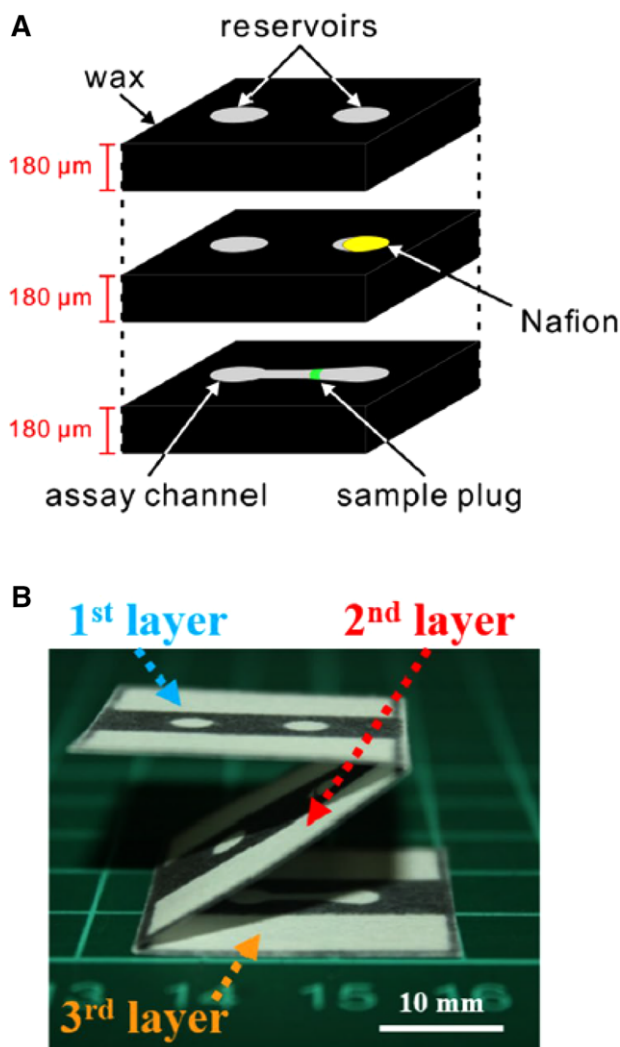


Figure 8. (A) Exploded view of μPAD structure and (B) Side view of folded μPAD layers. Reproduced from [127] with permission from Springer Nature.

was achieved for FITC-BSA spiked in human serum after 20 min using an applied voltage of 50 V [133]. This device was later coupled with lateral flow assay for the analysis of the β -subunit of the human chorionic gonadotropin (β -hCG) [134]. A tenfold enrichment was achieved for urine samples spiked with β -hCG after 20 min using a 9 V battery as an electric source and measuring the color reaction with a phone camera. One problem associated with ICP-based concentration methods is that the concentrated plug diffuses as soon as the voltage supply is stopped. To minimize this effect, Lee et al. designed a pop-up μ PAD that enable disconnecting the concentrated plug once the maximum enrichment was reached [135]. Orange G dye in 1 mM NaCl was enriched by 300-fold within 10 min using 100 V. The device design also included a wide outlet reservoir that is 9 mm in diameter to ensure continuous flow through the concentration time.

2.3.2 Other membranes

Marczak et al. [136] fabricated an ICP preconcentrator for simultaneous isolation and preconcentration of exosomes in biological samples. The microchannels were fabricated in polycarbonate sheets, and a cation-exchange membrane was integrated for the ICP. The samples containing exosomes were pneumatically injected into the sample channel, and then a transverse electric field was applied to force them out of the cross flow and into another channel, integrating with nanoporous membrane for concentrating exomes. The transverse channel was also filled with agarose gel to filter out unwanted cellular debris, and this device was used to capture 80% of exomes from cell culture media and blood serum samples.

2.3.3 Other approaches

Non-membrane approaches for ICP offer some advantages. Chun et al. presented a micro/nanofluidic device integrated with ESI-MS for peptide mixture detection. The microchip was fabricated with a borosilicate glass substrate by wet etching, an array of 63 μm wide, 10 nm deep nanochannels were also patterned by wet etching, connecting two microchannels. Peptide mixtures were preconcentrated using this device, and then were delivered to a spray tip using an integrated electrokinetic pump for ESI-MS analysis [137].

Faradaic ICP relies on bipolar electrodes to create ICP without the need to incorporate a NMI. Li et al. [138] demonstrated the enrichment of small molecules, DNA, protein, and nanoparticles with enrichment factors ranging from 200- to 500-fold within 5 min. The analytes were dissolved in 100 mM Tris-HClO₄ buffer (pH 8.1). The device comprised a U-shaped bipolar electrode. When voltage is applied, simultaneous oxidation of water produces H⁺ at the anode and OH⁻ at the cathode. The produced OH⁻ neutralizes cations in the buffer leading to ion depletion

zone at the cathodic side of the electrode. Sample ions can be enriched at this depletion zone similar to conventional ICP.

3 Extraction

3.1 Solid-phase extraction

Chromatographic preconcentration via SPE can be used to inject volumes larger than a single capillary/channel. This is largely beneficial when the number of samples and volumes to be analyzed are large. In order to maximize the analysis throughput, efficiency, and reduce analysis time, SPE can be performed in-line or online. This simply means that the extraction analysis is automated, enabling direct injection of samples, and excluding extensive manual sample pretreatment steps. To perform this, modification to some components in the instruments as well as in SPE are prerequisites.

3.1.1 In-line SPE-CE

In in-line SPE-CE, a preconcentration column is inserted (as an external short column) or synthesized (as a continuous porous column format) directly into the inlet end of the separation capillary. As a result, the extraction, enrichment, injection, and separation of compounds are conducted in the same capillary, eliminating further transfer of eluent. This allows automation of SPE-CE in commercial CE instruments. Packed beds filled with commercially available SPE materials in capillaries or microchip is one of the common designs for in-line SPE, whereby the interest in this mode has continued over the last 2 years. The packing of SPE materials inside a fused-silica capillary resembles the packing procedure of columns for capillary electrochromatography, either with the presence or the absence of frits to retain the material inside the capillary.

Due to sample amount limitation, matrix complexity and concentration issues for metabolic profiling using CE-MS, Pont et al. [139] inserted a C₁₈ sorbent-packed microcartridge in the separation capillary to facilitate separation and to enhance enrichment. The microcartridge (250 μm id) was inserted inside a separation capillary (75 μm id), at 7.5 cm from its inlet, using two plastic sleeves. The particles were retained using two frits (0.1 cm). However, the limited durability of the SPE microcartridge (complete clog) due to the complexity of the plasma matrix had forced them to change the SPE-CE-MS capillary each ten analysis.

Baciu et al. [140] constructed an SPE bed (capillary with 2 mm in length, 150 μm id, and 360 μm od) filled with OASIS HLB beads for the preconcentration of cocaine and its metabolites, prior to chiral CE separation. In order to be a fritless bed, the SPE bed was inserted into a PTFE sleeve, later sandwiched between two discontinued 50 μm id capillaries having length of 7.5 and 71.5 cm, respectively. The beads had to be 60 μm to be completely retained in the bed. The drugs were extracted at pH 9.1 where they were uncharged (cocaine

and (R,S)-methadone) or zwitterionic (6-acetylmorphine, benzoylecgonine, codein, and morphine). Efficient elution was achieved by using methanol acidified with acetic acid, such that the drugs were positively charged and thus easily desorbed from the SPE beads. Only 24 nL of the elution solvent was needed to completely desorb all analytes, inarguably a greener method to the offline SPE method. Enrichment factor values were not reported, nevertheless, low LOD values between 0.10 and 1.0 ng/mg were achieved; thanks to the advantage of injecting large volume of sample for 30 min at 930 mbar. Satisfactory recoveries ranging from 81 to 95% were obtained for all analytes. The same group constructed a similar SPE column for the preconcentration of racemic mephedrone and its metabolites, whereby LOD as low as 0.02 ng/mg was achieved for one of the enantiomer [141]. The similarity from both works was that the authors managed to minimize current instability and breakdown during the CE separation, a common issue when conducting in-line SPE using discontinuous packed bed in the same capillary with CE separation. They minimized it with the fine-tuning the elution volume (not more than 30 nL of elution solvent).

Monolithic SPE column, which also does not require frits, has been explored as preconcentrator for in-line SPE-CE. Espina-Benitez et al. [142] developed an in-line SPE system for the preconcentration and purification of molecules containing cis-diol in urine samples. The silica-based monolithic segment positioned at the inlet of the capillary was functionalized with a phenylboronic acid acrylamide derivative by photopolymerisation. After several exhaustive optimizations (e.g., concentration of monomer and co-monomer, concentration and type of photoinitiator, number of photografting steps, and irradiation time), they achieved highly efficient monoliths with an average minimum plate height of $8 \pm 2 \mu\text{m}$ at the optimum mobile phase velocity of $\sim 0.1 \text{ cm/s}$ (using catechol as model solute in frontal affinity chromatography). For a 1-cm monolithic column, they achieved retention factor of ~ 30 calculated with a dissociation equilibrium constant value of $\sim 290 \mu\text{M}$, 0.4 nmol/cm of active sites and

a dead volume of 40 nL. Percolation in a methanolic 100 mM phosphate solution (pH 8.5) was demonstrated to be optimal with respect to affinity and nonspecific interaction issues. A volume of 2.5 μL (which was translated as 20 times the monolith volume) can be percolated with a quantitative recovery yield ($\sim 100\%$) allowing preconcentration of catecholamines. As shown in Fig. 9, the in-line miniaturized boronate affinity monolithic column (μBAMC) was successfully implemented to analyze three catecholamines neurotransmitters (i.e., dopamine, adrenaline, and noradrenaline) in less than 2 μL of urine samples and within 10 min. Elution was performed with a small plug of acidic solution, allowing FASS prior in-line CZE separation at pH 8.75. This method was quantitatively sound for urine samples containing catecholamines with concentration between 10 and 400 ng/mL, with detection limit as low as 4.8 ng/mL (i.e., noradrenaline). A quantitative recovery of up to 103% was achieved in a single elution of 2.5 μL percolated catecholamines volume.

3.1.2 Online SPE-CE

Unlike in-line SPE-CE, online SPE has the column coupled to the CE system in an automated way, typically via an interface with flow-switching capabilities. Vial, valve, and T-piece are the most commonly used interfaces for online SPE-CE. Zhang et al. [143] has developed an automated online SPE-CE-UV system by using a four-port nano-valve as the interface, with LODs between 2.22 and 3.35 ng/mL providing about 20-fold improvement in comparison to direct CE-UV injection. The online procedure consisted of the following steps: sampling, clean-up, elution, CE injection, CE separation, and SPE regeneration. First, 10 mL sample was introduced to the online SPE column (filled with Oasis HLB), then it was rinsed to remove impurities concentrated on the online SPE column together with the analytes. After the cleanup step, a six-port valve was switched to inject position to elute the analytes. Then a 10-nL elution plug was injected to the

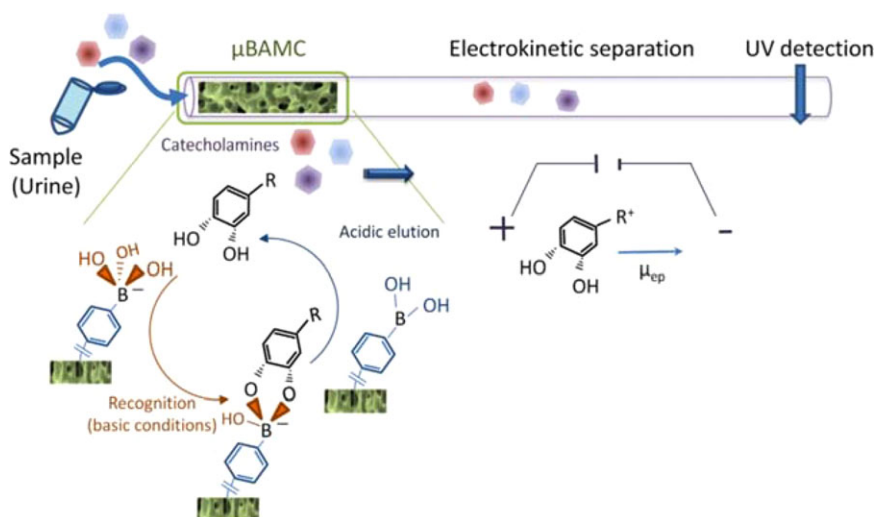


Figure 9. Schematic illustration of the different steps of cis-diols compounds analysis: preconcentration and purification on the integrated μBAMC unit, acidic elution, CZE separation and UV detection. Reprinted from [141] with permission.

CE capillary by switching the four-port nano-valve, and then the CE separation started. Finally, the two valves were returned to the original position, and the online SPE column was regenerated for the next analysis. The RSD for the peak area and migration time of the nano-valve injection mode were 1.6 and 1.8%, respectively, which were better than the direct pressure injection mode. All parameters were optimized including the four-port nano-valve position, sample volume, separation conditions, elution and sample loading flow rate, and four-port nano-valve switching time. This validated method with average recoveries ranged from 77.3 to 92.0% was applied for the analysis of sulfonamide antibiotics in wastewater.

Tascón et al. [144] developed an online-SPE-CE-MS method with LODs between 2 and 77 pg/mL, providing about 1000 times analytes-preconcentration in comparison to direct CE-MS. The C₁₈ sorbent Sep-pak packed microcartridge used for the online SPE was coupled between two pieces of separation capillary (7.5 and 52.5 cm) through the use of plastic sleeves built from peristaltic-pump Tygon® E-lab plastic tubing (Fig. 10). The packed material was confined within microcartridge between two frits. The online procedure involved the following steps: 115 µL of sample was introduced to the microcartridge for 20 min, then rinsed with the BGE for 2 min to eliminate the nonretained molecules and to equilibrate the separation capillary before the elution, and finally the retained compounds were eluted and injected by the elution mixture for 10 s to form a 50 nL plug before the CE-MS separation take place. Hydrodynamic sample introduction at high pressure was recommended in this method to obtain this optimal preconcentration factor. The precision was 5.0–10.5% and 0.8–1.5% for peak areas and migration times, respectively. Even though recoveries percentages have not been mentioned by authors, the validated method was applied successfully for harmala alkaloids in algae *Undaria pinnatifida* reaching very low detection of alkaloids at part per trillion of dry algae.

3.2 Liquid-liquid extraction

LLE is a commonly employed sample pretreatment method to purify and preconcentrate analytes of interest in complex sample matrices. In recent years, increasing attention has been directed toward the miniaturization of LLE technique

to simplify the procedure, reduce the amount of organic solvent usage, and deal with tiny samples. Moreover, efforts to achieve a minimal volume of acceptor extract have also been made to obtain high extraction preconcentration factors.

Among recent works, liquid-phase microextraction based on supported liquid membrane (SLM) has gained considerable attention due to its cost effectiveness, low organic solvent consumption, and, most importantly, good sample clean-up efficacy. A comprehensive overview of the feasibility of directly coupling flat sheet-based SLMs to CE was previously reported by Kubáň and Boček [145]. Recently, Pantůčková and Kubáň [146] demonstrated the simultaneous analysis of basic and acidic drugs present in urine samples. They used a tailor-made microextraction device compatible with commercial CE instruments. The device consisted of a sample and acceptor unit, which were separated by a flat polypropylene membrane immobilized with an organic solvent. Extracted analytes were injected from the membrane surface directly into a separation capillary for effective CE separation and quantification. The whole procedure, including extraction, injection, separation, and quantification, was fully automated in the CE system and the only manual procedures were preparing the SLM microextraction device and filling up the sample and acceptor solutions. The microdevice was discarded after each extraction, thereby eliminating sample carry over and tedious SLM regeneration steps.

Several new micro-LLE approaches have been introduced. Kubáň [147] reported a multiple-phase micro-electromembrane extraction approach using a free liquid membrane (FLM) as a selective phase interface between the aqueous sample and acceptor solution to facilitate the electrically induced transfer of charged species. The disposable micro-electromembrane extraction unit was filled with five consecutive plugs of immiscible aqueous and organic solutions; the aqueous sample formed the central phase and was encompassed by two FLMs and two extraction solutions. When electrical potential was applied at both ends, inorganic cations and anions in the sample solution migrated in opposite directions toward the corresponding FLM, crossed the FLM, and were quantitatively transferred to terminal extraction solutions. Simultaneously, the two FLMs selectively eliminated the migration of target analytes across the organic phases and the analytes were retained in the sample, which was then used for analysis. The resulting salt-free aqueous samples were suitable for direct injections to most standard

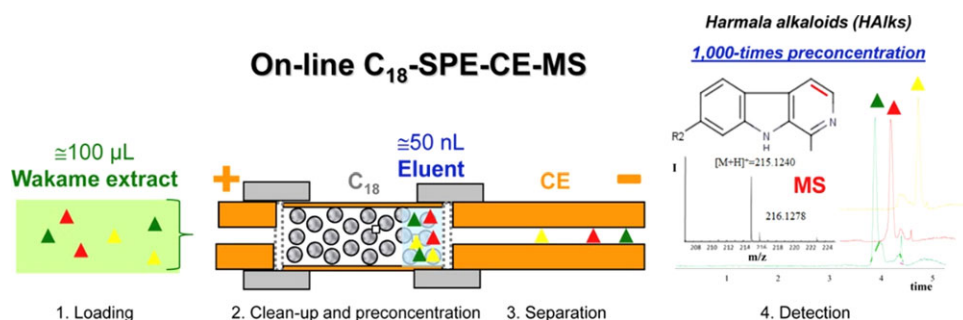


Figure 10. Schematic illustration of the online C₁₈ SPE-CE-MS system. The C₁₈ sorbent packed microcartridge was connected between the two pieces of separation capillary contained by two frits. Reprinted from [143] with permission.

analytical systems and are potentially suitable for online coupling with CE analysis.

Chui and co-workers [148] proposed a new variation of the FLM approach by direct in-line coupling of FLM extraction into an electrokinetic supercharging strategy to enhance online preconcentration efficiency in CE. A small plug of water-immiscible organic solvent (approximately 1 mm plug length) was introduced into the capillary inlet tip. Sample extraction/injection was subsequently performed by electrokinetically introducing the analytes from the sample solution across the selective phase interface FLM plug into the leading electrolyte plug. A small volume of terminating electrolyte was subsequently injected hydrodynamically into the capillary, followed by the application of voltage for effective separation and detection. This approach was applied for the determination of paraquat and diquat in polluted river water samples, and achieved superior sensitivity enhancement factors ranging from 1500- to 1866-fold when compared to the typical pressure injection in CE. No offline sample pretreatment step (except for the sample dilution) was required in this reported new approach.

Alhusban and co-workers [149, 150] developed an automated platform for online, near real-time monitoring of suspension cultures by integrating microfluidic components for cell counting and sample clean-up with high resolution CE. A microfluidic H-filter was used to isolate small molecules from a suspension culture allowing it to be injected into a sequential injection CE system. The developed system was successfully applied for the analysis of the metabolic biomarkers glucose, glutamine, leucine/isoleucine, and lactate from media as well as to study the metabolic effects of the drugs rotenone, β -lapachone, and clioquinol using lactate as metabolic indicator.

The integration of a sample preparation technique into a microchip electrophoresis system is a challenging task, as it involves multiple preprocessing steps. Although LLE is one of the most used sample preparation techniques prior to analysis with high resolution separation techniques, the integration of an LLE-based sample pretreatment technique in miniaturized electrophoretic separation systems remains limited. Recently, Hu et al. [151] reported a combined two-phase laminar flow LLE with electrophoretic separation on one glass microchip. Figure 11 shows a schematic diagram of the extraction unit and microchip design. The proposed system was successfully used to detect sanguinarine present in the spiked plasma and blood samples. Overall, the sample pretreatment steps were simplified, as no multi-vortex oscillation and centrifugation were needed. In addition, the integration of extraction with electrophoretic analysis did not require any auxiliary instrumentation.

4 Combinations of Stacking Methods

The combination of more than one online sample concentration technique is referred to as multistacking or hyphenated stacking. This can be performed sequentially when one

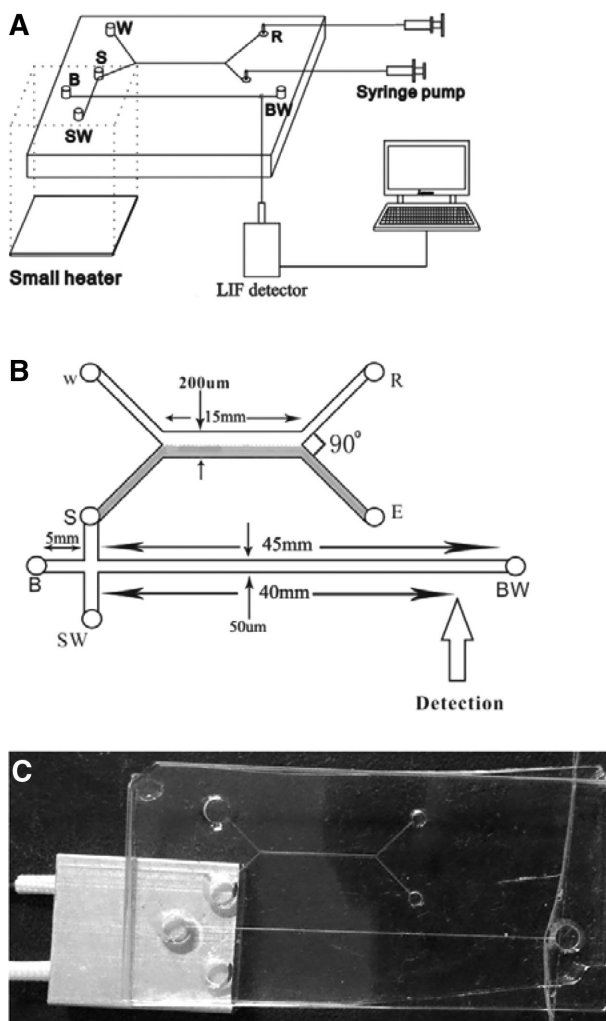


Figure 11. (A) Schematic diagram of the extract-CE glass chip; (B) top view of the chip, the grey part of channels is hydrophobic while the other parts are hydrophilic; (C) a photo of the extraction-CE microchip. Reproduced from [151] with permission.

stacking mode is preceded by another, or synergistically when the different stacking modes occur simultaneously. The amount of sample that can be injected when combining two different approaches normally extends beyond the amount achieved with just one. Furthermore, the use of two stacking modes can sharpen the analyte peaks and this leads to a clearer and more informative electropherogram. As such, the multiple stacking can be regarded as online sample preparation where the stacking strategy selectively removes interferences and enriches the analytes [13, 152, 153]. Multi-stacking of three and more techniques is possible, although the practical integration has some challenges [154, 155].

4.1 FASS/FASI-sweeping

To combine field enhancement with sweeping, the sample is prepared in a low conductivity solution devoid of

pseudostationary phase and this solution is injected into the capillary filled with BGE containing a pseudophase. FASS-sweeping was applied for the determination of catecholamines [156], steroid hormones [157], biogenic amines [158], deferoxamine [159], and cephalosporin antibiotics [160]. The urine and surface water samples were extracted by LLE and SPE prior to evaporation of the extract to dryness and reconstitution in a low conductivity sample diluent that was free of pseudostationary phase. Hydrodynamic injection of the prepared samples was performed for 50 to 100 s at 30–1000 mbar into a capillary containing the micellar BGE. Upon application of voltage, the analytes were stacked by field enhancement and sweeping prior electrochromatographic separation with UV and LIF detection.

Ionic liquids were investigated as alternative to the commonly used cationic CTAB pseudostationary phase for the separation of four catecholamines and four steroid hormones [156, 157]. The rationale for the use of imidazole-based ionic liquids was that these molecules offer additional chemical interaction (e.g., π - π and hydrophobic interactions) with the analyte and these interactions can be used to further improve the sensitivity enhancement factor. The studied ionic liquids were 1-dodecyl-3-methylimidazolium chloride (12 C-chain length) and 3-methyl-1-cetylimidazolium chloride (16 C-chain length). The concentration of ionic liquid was 0.5 mM for 3-methyl-1-cetylimidazolium chloride and 7 mM for 1-dodecyl-3-methylimidazolium. Indeed, the longer chain ionic liquid provided better analytical performance values than the shorter chain ionic liquid and CTAB. This multistacking strategy using ionic liquids provided SEF values of up to 85 and enabled limit of detection as low as 50 ng/mL. In addition to the improved SEFs, the authors further explored the use of ionic liquids as buffer additives in MEKC and for covalent modification of the capillary wall where the use of the ionic liquids were shown to improve the separation efficiency [158, 161].

Sensitive analysis of two antibiotics cefalexin and cefadroxil in surface water was achieved by sample clean up using offline SPE, fluorescence derivatisation with fluorescamine, and online stacking by reversed electrode polarity stacking mode (REPSM)-sweeping prior MEKC with LIF detection [160]. In REPSM, a reversed voltage is used to pump out the sample matrix from the capillary after a long hydrodynamic sample injection [162]. The use of this sample matrix removal step enables higher sample loads than there are typically obtained by FASS. Furthermore, this step also resulted in the first stacking process of the negatively charged analytes. However, the current has to be monitored closely and when reaching 97–99% of the BGE current, the polarity is switched for the separation to proceed. REPSM was integrated by preparing the sample in dilute borate buffer (i.e., 8 mM borate at pH of 8.2) and this solution was injected to fill the whole capillary. The BGE was 30 mM borate at pH 9.25 containing 2% 2-(2-hydroxypropyl)- β -cyclodextrin as the pseudophase for sweeping. Sweeping proceeded during REPSM, when the cyclodextrins from BGE in the outlet vial migrated with the EOF toward the capillary inlet and swept through the oppositely migrating anionic analytes. The

REPSM-sweeping strategy was compared to FASS-sweeping (without polarity reversal) and using a shorter sample injection for 0.6 min at 30 mbar. Figure 12 shows the electropherograms: (A) FASS-sweeping and (B and C) REPSM-sweeping. The analyte concentration in Fig. 12A and B was 1400 ng/L and in Fig. 12C was 60 ng/L. An approximately 25-fold improvement was achieved by REPSM-sweeping compared to the FASS-sweeping. This improvement was required to reach relevant trace level detection limits of the antibiotics in water samples (low ng/L-range). The analytical workflow of SPE-LVSS-sweeping method achieved LODs of 4.9 and 7.5 ng/L for cefalexin and cefadroxil, respectively, with a starting sample volume of 50 mL water sample. The sensitivity values were also comparable to more sophisticated and complicated HPLC-MS/MS instrumentation.

Eight β -adrenergic agonists (albuterol, cimaterol, clenbuterol, colterol, terbutaline, tulbuterol, ractopamine, and zilpaterol) were analyzed using a dialkyl anionic surfactant as novel pseudostationary phase for MEKC and sweeping [110]. This pseudostationary phase has a double hydrophobic carbon tail that can increase the partitioning with the analyte and thus improved the resolution and sensitivity compared to widely used SDS micelles. The sample injection regimen was a short plug of water (i.e., 10 s, 1 psi) prior to electrokinetic injection for 200 s at 10 kV. The BGE consisted of 50 mM NaH_2PO_4 at pH 2.5 containing 10 mM dialkyl anionic surfactant and 20% methanol. The sweeping buffer was 50 mM NaH_2PO_4 at pH 2.5 containing 80 mM surfactant and 30% methanol. High SEFs of up to 2000 and LODs of 5 ng/mL were achieved. The method was evaluated on animal feed samples.

FASS-sweeping was also applied to deferoxamine and deferiprone in whole blood [163], 5-nitroimidazoles in egg samples [164], chlorpheniramine in rat plasma [165], methamphetamine in hair samples [166], and glycopyrrolate

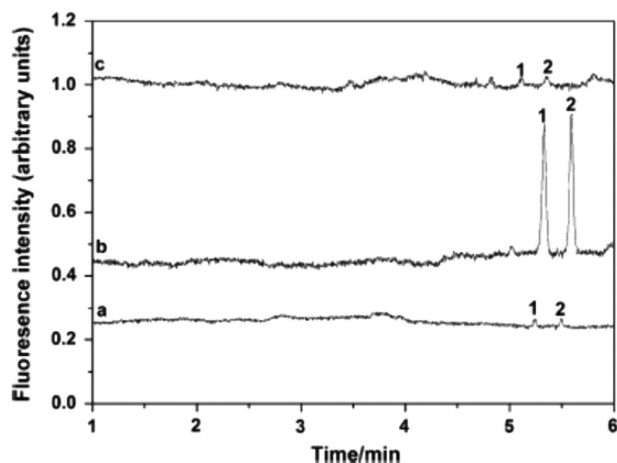


Figure 12. Electropherograms from the analysis of cefalexin (peak 1) and cefadroxil (peak 2) obtained by (A) FASS-sweeping and (B and C) REPSM-sweeping. The analyte concentration in (A, B) and (C) was 1400 ng/L and 60 ng/L, respectively. Reproduced from [160] with permission.

stereoisomers in rat plasma [167]. To suit the complex samples for FASI, an adequate procedure of sample preparation was required. For instance, dispersive micro-solid-phase extraction was explored for glycopyrrolate extraction of small plasma volumes (i.e., 50 μ L). FASI was then performed for at 10 to 18 kV for 1.5 to 10.5 min into a capillary conditioned with high conductivity BGE devoid of the pseudostationary phase. After injection, sweeping was induced by placing micellar BGE containing negatively charged SDS micelles [164, 167] or sulphated cyclodextrins [165, 166] at the both capillary ends. In addition to stacking by sweeping, the use of cyclodextrins also facilitated enantiomeric separation with baseline resolution of methamphetamine and chlorpheniramine. SEF values of 190 up to 10 000 were achieved which enabled trace analysis with detection limits of pg/mL to μ g/mL. For chlorpheniramine, the sensitive stacking strategy was beneficial to study the pharmacokinetic profile of the racemic drug orally administered to rats.

4.2 FASS/FASI-MSS

A simple way to integrate field enhancement and MSS is by preparing the sample in a diluent with organic solvent and using a higher conductivity BGE containing the surfactant. A different approach for the integration of FASS–MSS was reported by Liu and colleagues [168], where field amplification was in the low conductivity micellar sample solution. This was achieved by dissolving the sample in low conductivity micellar solution (i.e., 10 mM SDS) and injecting an acidic solution of (e.g., 35 mM H_3PO_4 with 60% acetonitrile) prior to the BGE (e.g., 30 mM Na_2HPO_4 at pH of 7.3). The application of separation voltage resulted in FASS and migration of the micelle bound analytes toward the organic solvent zone at the capillary inlet. At the boundary between these two zones, the decrease in the retention factor caused the release of the analytes due to the presence of high concentration of acetonitrile. The high pH difference between acidic solution and the BGE may also suggest the involvement of stacking by dynamic pH junction, causing high SEFs with this complex multi-stacking method. The SEFs for the antibiotics trimethoprim and sulfamethoxazole were 301 and 329, respectively. A similar method was applied for the analysis atenolol and metoprolol in human urine [169].

A portable microchip electrophoresis platform with C4D detection was explored for the determination of the anticancer drug tamoxifen including three of its metabolites [170] and vancomycin [171] in human serum using FASI–MSS. Mobility reversal was induced by injecting a micellar solution between the BGE and sample. When applied to serum, liquid–liquid extraction was performed, and the dried extract was reconstituted in sample diluent. Figure 13 shows the concentration of rhodamine 6G as model dye to visualize the stacking mechanism. The evolution of the stacked dye is shown in Fig. 13A–F at 15 to 20.8 s. The dye was electrokinetically introduced from two reservoirs (R1 and R3) filled with a low conductivity solution (i.e., 0.1 mM acetic acid in MeOH) into

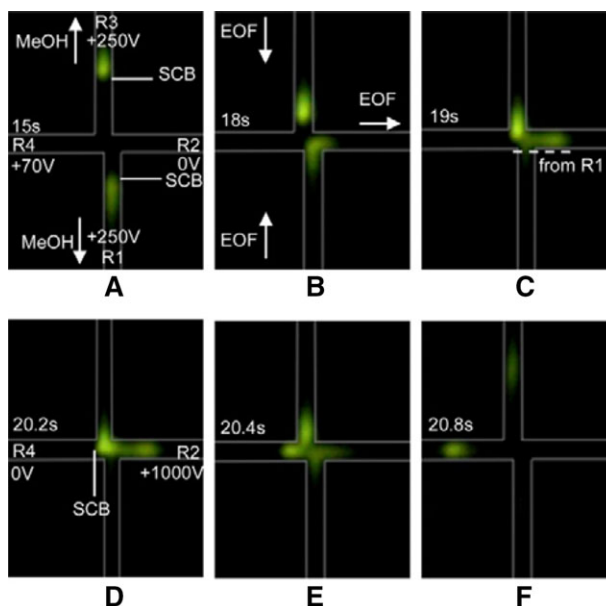


Figure 13. Multistacking by FASI–MSS in a T-shaped microfluidic chip. Evolution of the stacking zones depending on time (A–F). Rhodamine 6G was injected simultaneously from two streams (R1 and R3) prior to injection into the separation channel (R2 to R4). Reproduced from [171] with permission.

the channel containing the micellar solution (i.e., 10 mM SDS in 50 mM acetic acid). The dye migrated to the micellar solution where the dye molecules became bound to the micelles and the migration direction was reversed. At the boundary of sample diluent and micellar solution, the micelle-bound analyte was diluted which caused the release and stacking of the dye. This boundary migrated with the EOF toward the channel junction. At the junction and 20.4 s after the stacking process was started, the voltage was switched to 1 kV at R2 (R4 at ground) to inject the dye band into the separation channel. At this stage, a second focusing by the change in local electric field strength occurred because of the conductivity difference between BGE and dye band. The SEF for rhodamine 6G was 110 compared to typical gated injection. This method was then evaluated for the determination of tamoxifen fortified in human serum samples. The compact chip platform enabled fast detection of the analytes in less than 3 min but did require offline sample treatment as described above.

4.3 Sweeping–MSS

The mechanism of sweeping and MSS are opposite such that their combination is intuitive and potentially powerful. Sweeping–MSS can be achieved when the sample and BGE are both free of pseudostationary phase and a pseudostationary phase solution is injected between sample and BGE [172–174]. As with MSS, the pseudostationary phase must have an opposite charge to the analytes. Upon application of voltage, the pseudostationary phase collects the analyte molecules by sweeping and transport these molecules to the

micelle to solvent stacking boundary where dilution of the pseudostationary phase results in a release of the bound analyte. This process continues until the whole sample zone has been swept by the pseudostationary phase and the concentrated analytes are separated based on CZE.

A sweeping-MSS strategy for the determination of vanillic acid, ferulic acid, and cinnamic acid in plant extract from *Angelica sinensis*, a plant used in traditional Chinese medicine, was demonstrated [175]. The capillary was first filled with BGE (50 mM ammonium acetate at pH of 12.0 containing 50% methanol), then a volume of micellar solution (20 mM ammonium acetate containing 12 mM CTAB) followed by the sample (plant extract reconstituted in 20 mM ammonium acetate) and finally placing the capillary inlet in the BGE. Upon application of the voltage, the positively charged CTAB micelles migrated toward the capillary outlet and swept through the sample zone. The negatively charged analytes migrated in opposite direction to the micelles toward the capillary inlet. Once the analyte was bound to the micelles, the micelle-bound analytes were transported to the boundary of BGE containing 50% methanol for analyte release from the micelles. SEFs values of 42–77 and LODs of 0.05–0.06 $\mu\text{g/g}$ were obtained and the analyzed plant extract contained ferulic acid and cinnamic acid at 0.74 and 0.09 mg/g. Vanillic acid was not detected.

4.4 tITP-sweeping

To combine sweeping and tITP, a BGE containing a pseudostationary phase is used and the sample is devoid of this phase, with typically the ITP stage occurring prior to the pseudophase sweeping and separating the ITP-stacked analytes. tITP-sweeping was applied for the analysis of proteins [176] in artificial urine, bacteria in urine and blood [177], and seven hydrophobic chlorophenol residues in wines samples [178].

A fused silica capillary with two segments of different diameter and surface roughness was explored for the protein analysis of cytochrome c, ribonuclease, β -lactoglobulin, albumin, and amyloglucosidase [4]. The wider and rougher first segment was used to load large volumes of the high conductivity sample while the second segment was used for sweeping and MEKC separation. Using etching with supercritical water, a segment of wider diameter (i.e., 150–218 μm) was etched into the commercially available fused silica capillaries of 100 μm inner and 360 μm outer diameter. The etching process caused also an increase in surface roughness. The etched first segment of 15 cm length and 218 μm ID could accommodate up to 5.6 μL while the second segment remained unaltered. An advantage of using water as the etchant was that no residual impurities were obtained during the etching process that had to be removed by a post-process cleaning step. In an EOF suppressed approach, tITP and sweeping were integrated using a pseudostationary phase-free sample diluent (i.e., physiological saline solution) and a micellar BGE of 5% ethanol, 0.8% Brij 35, and 0.6% polyethylene glycol (Mw \sim 10000 g/mol). The sample conductivity values were

higher than the BGE, which would favor destacking in the electrophoretic separation. However, destacking was counteracted by tITP and sweeping. tITP and sweeping occurred simultaneously upon application of voltage. The increased capillary volume enabled higher sample loads of up to 3.7 μL . This method provided SEF values for the studied proteins of up to 196 and LODs of as low as 0.060 $\mu\text{g/mL}$. The use of a capillary with two segments of different diameter was also evaluated for bacterial analysis of *Escherichia coli* and *Staphylococcus aureus*. The combination of tITP-sweeping was suitable to focus the bacteria up to 680-fold and facilitated sensitive analysis of as little as \sim 14 injected bacteria cell (i.e., 2.8 μL sample injection with a bacteria concentration of \sim 5 \times 10³ cells/mL).

Sun et al. [178] developed a sophisticated method for the analysis of chlorophenols that are used as biocides in wine production. The chlorophenols were first extracted with DLLME followed by an eightfold diluted sample diluent (100 mM NaCl, 25% isopropanol, and 37% acetonitrile). The prepared sample was then injected into a capillary filled with micellar BGE (25 mM borate at pH of 11.2 containing 20% acetonitrile and 40 mM Brij-35) followed by micelle-free BGE. The underlying mechanism was proposed to be a result of tITP with ACN and dynamic pH-junction processes, however, the discontinuous micellar buffer system and sample prepared in a micellar-free solution also fulfilled the criteria for sweeping. The reported SEFs were 83–237, which was higher than the maximum SEF by sweeping alone. The maximum SEF by sweeping for the given sample injection of 20 cm or 33% of the total capillary length compared to typical injection (\sim 0.3 cm) would be a SEF of 67 (i.e., 20/0.3). Thus, the involvement of other stacking mechanism seems plausible. All seven analytes were baseline separated in less than 20 min and the method provided LODs of 5.5 to 16.0 ng/mL.

4.5 Dynamic pH junction—transient trapping

Zhang et al. [179] combined both dynamic pH junction and transient trapping by SDS micelles to enhance sensitivity of glutathione derivatives and amino acids in bacteria cells. The capillary was filled with alkaline BGE pH 9.5, followed by a sequence injection SDS in BGE, and a long sample plug at pH 4.5. Analytes were focused on the high pH boundary, followed by transient trapping due to the movement of SDS to the inlet. Transient trapping is sweeping in partial filling MEKC. The analytes are separated due to micelles after sweeping, and then migrate out of the pseudophase zone. This preconcentration process enhanced the detection of these ions in bacteria and HaCaT cells (*E. coli*, *Salmonella typhimurium*, and *Staphylococcus aureus*), by up to 430 reaching LODs of 10 pM by CE-LIF.

4.6 Electrokinetic supercharging

Electrokinetic supercharging (EKS) is a two-step stacking technique that employs tITP to preconcentrate analytes after a significantly long FASI [17, 180]. The technique is capable

of providing enrichment factors pronouncedly higher than either ITP or FASI can solely achieve [181, 182]. Since electrokinetic injection is utilized for sample loading during the FASI step, the technique exhibits a limited applicability to highly conductive sample matrices [183]. This shortcoming is usually overcome by applying a significant dilution for salty samples or performing a sample clean-up in order to minimize the detrimental effect of salt [184]. Chui et al. [148] exploited the integration of FLM with EKS for selective stacking of cationic herbicides in environmental samples. FLM–EKS is pretty similar to conventional EKS with the exception that a water-immiscible solvent plug is placed in front of the sample to satisfy the cleanup purpose during electrokinetic injection. The optimized FLM–EKS scheme was as follows: hydrodynamic injection of a plug (3% of the total capillary volume) of 20 mM potassium chloride as a LE followed by pressure injection of a short plug (0.1% of the total capillary volume) of tris(2-ethylhexyl) phosphate (TEHP) as FLM. The sample was then electrokinetically injected at 10 kV for 360 s. The FLM was pumped outside the capillary by applying a counter pressure of 50 mbar for 23.4 s, then a plug (2% of capillary volume) of 20 mM CTAB was injected as a TE. The integrated approach provided enhancement of detection sensitivity of up to 1800-fold compared to HDI and 2.5-fold over sole EKS and the LODs were down to 0.15 ng/mL.

Another limitation of the electrokinetic injection of sample is the movement of the stacking boundary during the long FASI step. Many approaches in the last 10 years were proposed for the immobilization of the stacking boundary through application of a counterflow (CF-EKS) [185–187] or employing the EOF to cease the movement of the stacking boundary [188–190]. Recently, the Chung's group revisited CF-EKS for the sensitive speciation of arsenic in water samples [191]. The authors applied a counter pressure (−0.2 psi) during electrokinetic injection (−20 kV for 3 min) of sample to immobilize the stacking boundary. Phosphate (100 mM) was employed as LE and 100 mM CHES was used as a TE. The CF-EKS enhanced the sensitivity by up to 45 000-fold. The LODs were down to 0.08–0.3 ng/L for standards and when applied to spring water samples spiked with arsenic species, the limit was 2–9 ng/L, which is attributed to the higher salinity and conductivity of the spring water samples [192].

EKS in its conventional form was investigated for the preconcentration of endocrine disrupting pollutants in water sample [193]. The authors used 100 mM NaCl as a LE, 100 mM CHES as a TE, and 12 mM borate as a BGE, and the samples were injected at −3 kV for 200 s. A 737-fold improvement when compared to conventional hydrodynamic injection was obtained and LODs were down to 4.9 µg/L for standards. In non-aqueous CE (NACE) environment, EKS was exploited for the determination and preconcentration of tamoxifen and its metabolites in human biological samples [194]. Potassium chloride (10 mM) was used as a LE and 10 mM pimozone as a TE and the sample was injected at 10 kV for 300 s. The NACE EKS method resulted in 600-fold enhancement in detection sensitivity and

the LODs were down to 50 ng/L, which allowed monitoring of target analytes in plasma samples from cancer patients.

5 Concluding Remarks

The necessity to achieve lower detection limits has remained and will continue to grow as the need to detect even lower amounts of chemicals increases. The last 2 years have seen a sustained effort in research in this area, and it is anticipated that this will continue. As expected for any mature technique, applications are becoming more prominent, but there are still many challenges remaining such that there is still a need for new methods to deal with the variety of targets and sample matrices. One of the greatest issues in all electrokinetic approaches is the susceptibility to variations in matrix composition, which ultimately compromise the concentration effect, and for many applications dictate the use of SPE or LLE. The inability to integrate and automate SPE and LLE with the simplicity of stacking, limits the appeal of these approaches.

M.C.B. thanks the Australian Research Council for a Future Fellowship (FT130100101). J.P.Q. thanks the Australian Research Council for the Discovery Grant DP180102810. H.H.S. thanks the Ministry of Education Malaysia for financial support through Fundamental Research Grant Scheme (FRGS) (R.J130000.7826.4F933). A.A.A. acknowledges the Deanship of Scientific Research and Graduate Studies at Al-Zaytoonah University of Jordan (2018-2017/28/19). W.G. thanks the National Science Centre Poland for a Doctoral Scholarship Etiuda (2016/20/T/NZ7/00266). A.W. thanks the University of Queensland for the UQ Development Fellowship (UQFEL1831057). A.S.A.K thanks the Ministry of Education Malaysia for financial support through a Research University Grant (Q.J130000.2526.16H14).

The authors have declared no conflict of interest.

6 References

- [1] Breadmore, M. C., *J. Chromatogr. A* 2012, 1221, 42–55.
- [2] Breadmore, M. C., *Electrophoresis* 2007, 28, 254–281.
- [3] Breadmore, M. C., Thabano, J. R., Dawod, M., Kazarian, A. A., Quirino, J. P., Guijt, R. M., *Electrophoresis* 2009, 30, 230–248.
- [4] Breadmore, M. C., Dawod, M., Quirino, J. P., *Electrophoresis* 2011, 32, 127–148.
- [5] Breadmore, M. C., Shallan, A. I., Rabanes, H. R., Gstoettenmayr, D., Abdul Keyon, A. S., Gaspar, A., Dawod, M., Quirino, J. P., *Electrophoresis* 2013, 34, 29–54.
- [6] Breadmore, M. C., Tubaon, R. M., Shallan, A. I., Phung, S. C., Abdul Keyon, A. S., Gstoettenmayr, D., Prapatpong, P., Alhusban, A. A., Ranjbar, L., See, H. H., Dawod, M., Quirino, J. P., *Electrophoresis* 2015, 36, 36–61.
- [7] Breadmore, M. C., Wuethrich, A., Li, F., Phung, S. C., Kalsoom, U., Cabot, J. M., Tehranirokh, M., Shallan, A. I., Abdul Keyon, A. S., See, H. H., Dawod, M., Quirino, J. P., *Electrophoresis* 2017, 38, 33–59.

- [8] Mala, Z., Krivankova, L., Gebauer, P., Bocek, P., *Electrophoresis* 2007, 28, 243–253.
- [9] Mala, Z., Slampova, A., Gebauer, P., Bocek, P., *Electrophoresis* 2009, 30, 215–229.
- [10] Mala, Z., Gebauer, P., Bocek, P., *Electrophoresis* 2011, 32, 116–126.
- [11] Slampova, A., Mala, Z., Pantuckova, P., Gebauer, P., Bocek, P., *Electrophoresis* 2013, 34, 3–18.
- [12] Mala, Z., Slampova, A., Krivankova, L., Gebauer, P., Bocek, P., *Electrophoresis* 2015, 36, 15–35.
- [13] Šlampová, A., Malá, Z., Gebauer, P., Boček, P., *Electrophoresis* 2017, 38, 20–32.
- [14] Aranas, A. T., Guidote, A. M. Jr., Quirino, J. P., *Anal. Bioanal. Chem.* 2009, 394, 175–185.
- [15] Chen, Y., Lü, W., Chen, X., Teng, M., *Cent. Eur. J. Chem.* 2012, 10, 611–638.
- [16] Chiu, T. C., *Anal. Bioanal. Chem.* 2013, 405, 7919–7930.
- [17] Dawod, M., Chung, D. S., *J. Sep. Sci.* 2011, 34, 2790–2799.
- [18] Giordano, B. C., Burgi, D. S., Hart, S. J., Terray, A., *Anal. Chim. Acta* 2012, 718, 11–24.
- [19] Hou, X., Zhang, X., Lu, Y., *Anal. Methods* 2017, 9, 10–17.
- [20] Kitagawa, F., Otsuka, K., *J. Chromatogr. A* 2014, 1335, 43–60.
- [21] Ramautar, R., Jong, G. J., Somsen, G. W., *Electrophoresis* 2012, 33, 243–250.
- [22] Ramautar, R., Somsen, G. W., de Jong, G. J., *Electrophoresis* 2014, 35, 128–137.
- [23] Ramautar, R., Somsen, G. W., de Jong, G. J., *Electrophoresis* 2010, 31, 44–54.
- [24] Ramautar, R., Somsen, G. W., de Jong, G. J., *Electrophoresis* 2016, 37, 35–44.
- [25] Sanchez-Hernandez, L., Castro-Puyana, M., Marina, M. L., Crego, A. L., *Electrophoresis* 2012, 33, 228–242.
- [26] Sanchez-Hernandez, L., Garcia-Ruiz, C., Luisa Marina, M., Luis Crego, A., *Electrophoresis* 2010, 31, 28–43.
- [27] Tempels, F. W., Underberg, W. J., Somsen, G. W., de Jong, G. J., *Electrophoresis* 2008, 29, 108–128.
- [28] Wen, Y., Li, J., Ma, J., Chen, L., *Electrophoresis* 2012, 33, 2933–2952.
- [29] Breadmore, M. C., Sängner-van de Griend, C. E., *LCGC North America* 2014, 32, 174–186.
- [30] Mikkers, F. E. P., Everaerts, F. M., Verheggen, T. P. E. M., *J. Chromatogr. A* 1979, 169, 11–20.
- [31] Burgi, D. S., Chien, R. L., *Anal. Chem.* 1991, 63, 2042–2047.
- [32] Kerrin, E. S., White, R. L., Quilliam, M. A., *Anal. Bioanal. Chem.* 2017, 409, 1481–1491.
- [33] Ciura, K., Pawelec, A., Buszewska-Forajta, M., Markuszewski, M. J., Nowakowska, J., Prah, A., Wielgomas, B., Dziomba, S., *J. Sep. Sci.* 2017, 40, 1167–1175.
- [34] Šesták, J., Thormann, W., *J. Chromatogr. A* 2017, 1502, 51–61.
- [35] Sestak, J., Thormann, W., *J. Chromatogr. A* 2017, 1512, 124–132.
- [36] Sestak, J., Theurillat, R., Sandbaumhuter, F. A., Thormann, W., *J. Chromatogr. A* 2018, 1558, 85–95.
- [37] Zhang, C. X., Meagher, M. M., *Anal. Chem.* 2017, 89, 3285–3292.
- [38] Zeid, A. M., Kaji, N., Nasr, J. J. M., Belal, F. F., Baba, Y., Walash, M. I., *J. Chromatogr. A* 2017, 1503, 65–75.
- [39] Xie, X., Yang, Y., Zhou, H., Li, M., Zhu, Z., *Talanta* 2018, 179, 822–827.
- [40] Oukacine, F., Geze, A., Choisnard, L., Putaux, J. L., Stahl, J. P., Peyrin, E., *Anal. Chem.* 2018, 90, 2493–2500.
- [41] Hamidi, S., Khoubnasabjafari, M., Ansarin, K., Jouyban-Gharamaleki, V., Jouyban, A., *Curr. Pharm. Anal.* 2016, 12, 137–145.
- [42] Sun, S., Wang, Y., Liu, X., Fu, R., Yang, L., *Talanta* 2018, 180, 90–97.
- [43] Forough, M., Farhadi, K., Eyshi, A., Molaei, R., Khalili, H., Javan Kouzegaran, V., Matin, A. A., *J. Chromatogr. A* 2017, 1516, 21–34.
- [44] Zhang, C., Bi, C., Clarke, W., Hage, D. S., *J. Chromatogr. A* 2017, 1523, 114–122.
- [45] Zhang, J., Sun, A., Yang, Y., Hu, J., Wei, L., Gao, B., Ding, X., Qin, Y., Sun, C., *Chromatographia* 2016, 79, 1649–1658.
- [46] Yi, J., Zeng, L., Wu, Q., Yang, L., Xie, T., *Food Anal. Methods* 2018, 11, 1608–1618.
- [47] Forough, M., Farhadi, K., Molaei, R., Khalili, H., Shakeri, R., Zamani, A., Matin, A. A., *J. Chromatogr. B* 2017, 1040, 22–37.
- [48] Moreno-Gonzalez, D., Krulisova, M., Gamiz-Gracia, L., Garcia-Campana, A. M., *Electrophoresis* 2018, 39, 608–615.
- [49] Diaz-Quiroz, C. A., Francisco Hernandez-Chavez, J., Ulloa-Mercado, G., Gortares-Moroyqui, P., Martinez-Macias, R., Meza-Escalante, E., Serrano-Palacios, D., *J. Chromatogr. B* 2018, 1092, 386–393.
- [50] White, B., Smyth, M. R., Lunte, C. E., *Anal. Methods* 2017, 9, 1248–1252.
- [51] Zheng, Y., Peng, X., Wu, Y., *Food Anal. Methods* 2018, 11, 1155–1162.
- [52] Li, M., Chen, X., Guo, Y., Zhang, B., Tang, F., Wu, X., *Electrophoresis* 2016, 37, 3109–3117.
- [53] Gladysz, M., Krol, M., Wozniakiewicz, M., Koscielniak, P., *Talanta* 2018, 184, 287–295.
- [54] Hong, Y.-Q., Guo, X., Chen, G.-H., Zhou, J.-W., Zou, X.-M., Liao, X., Hou, T., *J. Food Safety* 2017, 38, e12382.
- [55] Polikarpova, D., Makeeva, D., Kartsova, L., Dolgonosov, A., Kolotilina, N., *Talanta* 2018, 188, 744–749.
- [56] Chen, Z., Bi, X., Li, J., Tang, Y., Fan, G., Sun, D., *J. Sep. Sci.* 2016, 39, 440–449.
- [57] Zhang, Y., Zhang, Y., Yu, S., Zhang, Y., Zhu, L., He, P., Wang, Q., *Microfluid. Nanofluid.* 2017, 21, 97.
- [58] Islas, G., Rodriguez, J. A., Perez-Silva, I., Miranda, J. M., Ibarra, I. S., *J. Anal. Methods Chem.* 2018, 2018, 5394527.
- [59] Moreno-Gonzalez, D., Lupion-Enriquez, I., Garcia-Campana, A. M., *Electrophoresis* 2016, 37, 1212–1219.
- [60] Chen, M., Huang, Y., Xu, L., Zhang, H., Zhang, G., Chen, A., *Biomed. Chromatogr.* 2018, 32, e4125.

- [61] Yu, H. X., Hao, Z. Y., Li, L., Huang, Y. Y., Zhang, H. F., Chen, A. J., *Int. J. Anal. Chem.* 2017, 2017, 3813879.
- [62] Kalaycıođlu, Z., Erim, F. B., *Food Anal. Methods* 2016, 9, 706–711.
- [63] Patel, A. V., Kawai, T., Wang, L., Rubakhin, S. S., Sweedler, J. V., *Anal. Chem.* 2017, 89, 12375–12382.
- [64] Tuma, P., Heneberg, P., Vaculin, S., Koval, D., *Electrophoresis* 2018, 39, 2605–2611.
- [65] Malinina, J., Kamencev, M., Tkach, K., Yakimova, N., Kuchumova, I., Moskvin, L., *Microchem. J.* 2018, 137, 208–213.
- [66] Kitagawa, F., Kinami, S., Takegawa, Y., Nukatsuka, I., Sueyoshi, K., Kawai, T., Otsuka, K., *Electrophoresis* 2017, 38, 380–386.
- [67] Crosnier de Lassichere, C., Mai, T. D., Otto, M., Taverna, M., *Anal. Chem.* 2018, 90, 2555–2563.
- [68] Kitagawa, F., Ishiguro, T., Tateyama, M., Nukatsuka, I., Sueyoshi, K., Kawai, T., Otsuka, K., *Electrophoresis* 2017, 38, 2075–2080.
- [69] Wu, X., Xu, Z., Huang, Z., Shao, C., *Electrophoresis* 2016, 37, 2963–2969.
- [70] Rohde, A., Hammerl, J. A., Appel, B., Dieckmann, R., Al Dahouk, S., *Food Microbiol.* 2015, 46, 395–407.
- [71] Phung, S. C., Cabot, J. M., Macka, M., Powell, S. M., Guijt, R. M., Breadmore, M., *Anal. Chem.* 2017, 89, 6513–6520.
- [72] Moreno-Gordaliza, E., van der Lee, S. J., Demirkan, A., van Duijn, C. M., Kuiper, J., Lindenburg, P. W., Hanke-meier, T., *Anal. Chim. Acta* 2016, 944, 57–69.
- [73] Mai, T. D., Oukacine, F., Taverna, M., *J. Chromatogr. A* 2016, 1453, 116–123.
- [74] Schoch, R. B., Ronaghi, M., Santiago, J. G., *Lab Chip* 2009, 9, 2145–2152.
- [75] Persat, A., Marshall, L. A., Santiago, J. G., *Anal. Chem.* 2009, 81, 9507–9511.
- [76] Eid, C., Santiago, J. G., *Analyst* 2017, 142, 48–54.
- [77] Eid, C., Branda, S. S., Meagher, R. J., *Analyst* 2017, 142, 2094–2099.
- [78] van Kooten, X. F., Truman-Rosentsvit, M., Kaigala, G. V., Bercovici, M., *Sci. Rep.* 2017, 7, 10467.
- [79] Sydes, D., Kler, P. A., Zipfl, P., Lutz, D., Bouwes, H., Huhn, C., *Sens. Actuators B* 2017, 240, 330–337.
- [80] Hradski, J., Chorvathova, M. D., Bodor, R., Sabo, M., Matejcek, S., Masar, M., *Anal. Bioanal. Chem.* 2016, 408, 8669–8679.
- [81] Marczak, S., Senapati, S., Slouka, Z., Chang, H. C., *Biosens. Bioelectron.* 2016, 86, 840–848.
- [82] Marczak, S., Smith, E., Senapati, S., Chang, H. C., *Electrophoresis* 2017, 38, 2592–2602.
- [83] Loessberg-Zahl, J., Janssen, K. G., McCallum, C., Gillespie, D., Pennathur, S., *Anal. Chem.* 2016, 88, 6145–6150.
- [84] Rosenfeld, T., Bercovici, M., *Lab Chip* 2018, 18, 861–868.
- [85] Zeidman Kalman, T., Khalandovsky, R., Tenenbaum Gonenman, E., Bercovici, M., *Angew. Chem. Int. Ed.* 2018, 57, 3343–3348.
- [86] Hattori, T., Okamura, H., Asaoka, S., Fukushi, K., *J. Chromatogr. A* 2017, 1511, 132–137.
- [87] Fukushi, K., Fujita, Y., Nonogaki, J., Tsujimoto, J. I., Hattori, T., Inui, H., Beskoski, V. P., Hotta, H., Hayashi, M., Nakano, T., *Anal. Bioanal. Chem.* 2018, 410, 1825–1831.
- [88] Crevillén, A. G., de Frutos, M., Diez-Masa, J. C., *Microchem. J.* 2017, 133, 600–606.
- [89] Aebersold, R., Morrison, H. D., *J. Chromatogr.* 1990, 516, 79–88.
- [90] Britz-McKibbin, P., Bebault, G. M., Chen, D. D., *Anal. Chem.* 2000, 72, 1729–1735.
- [91] Fan, Y., Li, S., Fan, L., Cao, C., *Talanta* 2012, 95, 42–49.
- [92] Yang, Q., Fan, L. Y., Huang, S. S., Zhang, W., Cao, C. X., *Electrophoresis* 2011, 32, 1015–1024.
- [93] Zhu, G., Sun, L., Dovichi, N. J., *Analyst* 2016, 141, 5216–5220.
- [94] Zhang, Z., Zhu, G., Peuchen, E. H., Dovichi, N. J., *Microchim. Acta* 2017, 184, 921–925.
- [95] Chen, D., Shen, X., Sun, L., *Analyst* 2017, 142, 2118–2127.
- [96] Chen, D., Shen, X., Sun, L., *Anal. Chim. Acta* 2018, 1012, 1–9.
- [97] Zhao, Y., Sun, L., Zhu, G., Dovichi, N. J., *J. Proteome Res.* 2016, 15, 3679–3685.
- [98] Lubeckyj, R. A., McCool, E. N., Shen, X., Kou, Q., Liu, X., Sun, L., *Anal. Chem.* 2017, 89, 12059–12067.
- [99] McCool, E. N., Lubeckyj, R. A., Shen, X., Chen, D., Kou, Q., Liu, X., Sun, L., *Anal. Chem.* 2018, 90, 5529–5533.
- [100] Yasuno, K., Fukushi, K., *Electrophoresis* 2016, 37, 2496–2501.
- [101] Terabe, S., Otsuka, K., Ichikawa, K., Tsuchiya, A., Ando, T., *Anal. Chem.* 1984, 56, 111–113.
- [102] Yue-Qin, H., Xin, G., Guan-Hua, C., Jia-Wei, Z., Xue-Mei, Z., Xue, L., Ting, H., *J. Food Safety* 2018, 38, e12382.
- [103] Chang, P. L., Hsieh, M. M., Chiu, T. C., *Int. J. Environ. Res. Public Health* 2016, 13, 409.
- [104] Quirino, J. P., Terabe, S., *Science* 1998, 282, 465–468.
- [105] Quirino, J. P., Haddad, P. R., *Anal. Chem.* 2008, 80, 6824–6829.
- [106] Quirino, J. P., *J. Chromatogr. A* 2009, 1216, 294–299.
- [107] Guidote, A. M., Jr., Quirino, J. P., *J. Chromatogr. A* 2010, 1217, 6290–6295.
- [108] Quirino, J. P., Grochocki, W., Markuszewski, M. J., *Anal. Chem.* 2017, 89, 13422–13428.
- [109] Wu, T., Yu, C., Li, R., Li, J., *Instrum. Sci. Technol.* 2018, 46, 364–386.
- [110] Hsieh, S. Y., Wang, C. C., Kou, H. S., Wu, S. M., *J. Pharm. Biomed. Anal.* 2017, 141, 222–228.
- [111] Tejada-Casado, C., Moreno-Gonzalez, D., Del Olmo-Iruela, M., Garcia-Campana, A. M., Lara, F. J., *Talanta* 2017, 175, 542–549.
- [112] Rahim, K. A., Sanagi, M. M., Hermawan, D., Ibrahim, W. A. W., Keyon, A. S. A., *Malays. J. Anal. Sci.* 2018, 22, 54–63.
- [113] Chen, S. Y., Chen, W. C., Chang, S. Y., *J. Sep. Sci.* 2018, 41, 1871–1879.

- [114] Shi, L., Wang, J., Feng, J., Zhao, S., Wang, Z., Tao, H., Liu, S., *J. Sep. Sci.* 2017, 40, 2662–2670.
- [115] Su, R., Li, D., Wu, L., Han, J., Lian, W., Wang, K., Yang, H., *J. Sep. Sci.* 2017, 40, 2950–2958.
- [116] Pyell, U., Rageh, A. H., El-Awady, M., *Chromatographia* 2017, 80, 359–382.
- [117] Yang, Q., Chen, B., He, M., Hu, B., *Talanta* 2018, 186, 88–96.
- [118] Wei, J. C., Hu, J., Cao, J. L., Wan, J. B., He, C. W., Hu, Y. J., Hu, H., Li, P., *J. Agric. Food Chem.* 2016, 64, 932–940.
- [119] Sanuki, R., Sueyoshi, K., Endo, T., Hisamoto, H., *Anal. Chem.* 2017, 89, 6505–6512.
- [120] Boublik, M., Riesova, M., Dubsy, P., Gas, B., *Electrophoresis* 2018, 39, 1390–1398.
- [121] Chao, H. C., Liao, H. W., Kuo, C. H., *J. Chromatogr. A* 2016, 1445, 149–157.
- [122] Wuethrich, A., Quirino, J. P., *J. Sep. Sci.* 2017, 40, 927–932.
- [123] Aturki, Z., Fanali, S., Rocco, A., *Electrophoresis* 2016, 37, 2875–2881.
- [124] Tubaon, R. M., Haddad, P. R., Quirino, J. P., *Anal. Chem.* 2017, 89, 13058–13063.
- [125] Chen, Y. Y., Chiu, P. H., Weng, C. H., Yang, R. J., *Biomicrofluidics* 2016, 10, 014119.
- [126] Kim, W., Park, S., Kim, K., Kim, S. J., *Lab Chip* 2017, 17, 3841–3850.
- [127] Chou, K. H., Yeh, S. H., Yang, R. J., *Microfluid. Nanofluid.* 2017, 21, 112.
- [128] Son, S. Y., Lee, H., Kim, S. J., *Micro Nano Syst. Lett.* 2017, 5, 8.
- [129] Liu, N., Phan, D. T., Lew, W. S., *IEEE Trans. Biomed. Circuits Syst.* 2017, 11, 1392–1399.
- [130] Yeh, S. H., Chou, K. H., Yang, R. J., *Lab Chip* 2016, 16, 925–931.
- [131] Gao, H., Xie, M. R., Liu, J. J., Fang, F., Wu, Z. Y., *Microfluid. Nanofluid.* 2018, 22, 50.
- [132] Han, S. I., Hwang, K. S., Kwak, R., Lee, J. H., *Lab Chip* 2016, 16, 2219–2227.
- [133] Han, S. I., Yoo, Y. K., Lee, J., Kim, C., Lee, K., Lee, T. H., Kim, H., Yoon, D. S., Hwang, K. S., Kwak, R., Lee, J. H., *Sensors and Actuators, B: Chemical* 2018, 268, 485–493.
- [134] Kim, C., Yoo, Y. K., Han, S. I., Lee, J., Lee, D., Lee, K., Hwang, K. S., Lee, K. H., Chung, S., Lee, J. H., *Lab Chip* 2017, 17, 2451–2458.
- [135] Lee, K., Yoo, Y. K., Han, S. I., Lee, J., Lee, D., Kim, C., Lee, J. H., *Micro Nano Syst. Lett.* 2017, 5, 11.
- [136] Marczak, S., Richards, K., Ramshani, Z., Smith, E., Senapati, S., Hill, R., Go, D. B., Chang, H. C., *Electrophoresis* 2018, 39, 2029–2038.
- [137] Chun, H., *J. Chromatogr. A* 2018, 1543, 67–72.
- [138] Li, X., Luo, L., Crooks, R. M., *Anal. Chem.* 2017, 89, 4294–4300.
- [139] Pont, L., Benavente, F., Jaumot, J., Tauler, R., Alberch, J., Gines, S., Barbosa, J., Sanz-Nebot, V., *Electrophoresis* 2016, 37, 795–808.
- [140] Baciú, T., Borrull, F., Aguilar, C., Calull, M., *J. Pharm. Biomed. Anal.* 2016, 131, 420–428.
- [141] Baciú, T., Borrull, F., Calull, M., Aguilar, C., *Electrophoresis* 2016, 37, 2352–2362.
- [142] Espina-Benitez, M. B., Randon, J., Demesmay, C., Dugas, V., *J. Chromatogr. A* 2017, 1494, 65–76.
- [143] Zhang, Z., Lin, L., Zhang, X., *Chromatographia* 2017, 80, 127–135.
- [144] Tascon, M., Gagliardi, L. G., Benavente, F., *Anal. Chim. Acta* 2017, 954, 60–67.
- [145] Kuban, P., Bocek, P., *J. Chromatogr. A* 2014, 1346, 25–33.
- [146] Pantuckova, P., Kuban, P., *J. Chromatogr. A* 2017, 1519, 137–144.
- [147] Kuban, P., *Anal. Chem.* 2017, 89, 8476–8483.
- [148] Chui, M. Q., Thang, L. Y., See, H. H., *J. Chromatogr. A* 2017, 1481, 145–151.
- [149] Alhusban, A. A., Breadmore, M. C., Gueven, N., Guijt, R. M., *Anal. Chim. Acta* 2016, 920, 94–101.
- [150] Alhusban, A. A., Breadmore, M. C., Gueven, N., Guijt, R. M., *Sci. Rep.* 2017, 7, 10337.
- [151] Hu, Y., Peng, H., Yan, Y., Guan, S., Wang, S., Li, P. C. H., Sun, Y., *Anal. Chim. Acta* 2017, 985, 121–128.
- [152] Wuethrich, A., Haddad, P. R., Quirino, J. P., *Trends Anal. Chem.* 2016, 80, 604–611.
- [153] Wuethrich, A., Haddad, P. R., Quirino, J. P., *J. Chromatogr. A* 2015, 1401, 84–88.
- [154] Grochocki, W., Markuszewski, M. J., Quirino, J. P., *J. Chromatogr. A* 2015, 1424, 111–117.
- [155] Grochocki, W., Markuszewski, M. J., Quirino, J. P., *J. Chromatogr. A* 2016, 1442, 140–143.
- [156] Bessonova, E., Kartsova, L., Gallyamova, V., *J. Sep. Sci.* 2017, 40, 2304–2311.
- [157] Bessonova, E. A., Kartsova, L. A., Gallyamova, V. F., *J. Anal. Chem.* 2016, 71, 696–702.
- [158] Kolobova, E. A., Kartsova, L. A., Bessonova, E. A., Kravchenko, A. V., *Analitika i Kontrol* 2017, 21, 57–64.
- [159] Lin, H. J., Hsieh, K. P., Chiou, S. S., Kou, H. S., Wu, S. M., *J. Pharm. Biomed. Anal.* 2016, 131, 497–502.
- [160] Rageh, A. H., Klein, K. F., Pyell, U., *Chromatographia* 2016, 79, 225–241.
- [161] Kolobova, E., Kartsova, L., Kravchenko, A., Bessonova, E., *Talanta* 2018, 188, 183–191.
- [162] Liu, Z., Sam, P., Sirimanne, S. R., McClure, P. C., Grainger, J., Patterson, D. G. Jr., *J. Chromatogr. A* 1994, 673, 125–132.
- [163] Lin, H. J., Kou, H. S., Chiou, S. S., Wu, S. M., *Electrophoresis* 2016, 37, 2091–2096.
- [164] Airado-Rodriguez, D., Hernandez-Mesa, M., Garcia-Campana, A. M., Cruces-Blanco, C., *Food Chem.* 2016, 213, 215–222.
- [165] Yao, Y., Zhou, L., Li, M., Guo, X., *J. Pharm. Biomed. Anal.* 2018, 148, 142–148.
- [166] Mikuma, T., Iwata, Y. T., Miyaguchi, H., Kuwayama, K., Tsujikawa, K., Kanamori, T., Kanazawa, H., Inoue, H., *Electrophoresis* 2016, 37, 2970–2976.

- [167] Liu, Y., Yu, L., Zhang, H., Chen, D., *J. Sep. Sci.* 2018, *41*, 1395–1404.
- [168] Liu, L., Wan, Q., Xu, X., Duan, S., Yang, C., *Food Chem.* 2017, *219*, 7–12.
- [169] Wan, Q., Liu, Y., Yang, C., Liu, L., *Anal. Chim. Acta* 2017, *978*, 61–67.
- [170] Thang, L. Y., See, H. H., Quirino, J. P., *Anal. Chem.* 2016, *88*, 9915–9919.
- [171] Chong, K. C., Thang, L. Y., Quirino, J. P., See, H. H., *J. Chromatogr. A* 2017, *1485*, 142–146.
- [172] Quirino, J. P., *J. Chromatogr. A* 2010, *1217*, 7776–7780.
- [173] Quirino, J. P., Guidote, A. M. Jr., *J. Chromatogr. A* 2011, *1218*, 1004–1010.
- [174] Wuethrich, A., Haddad, P. R., Quirino, J. P., *Electrophoresis* 2016, *37*, 1122–1128.
- [175] Yang, X., Hao, L., Zhang, S., Wang, C., Wang, Z., *RSC Adv.* 2018, *8*, 7949–7955.
- [176] Horka, M., Karasek, P., Roth, M., Slais, K., *Electrophoresis* 2017, *38*, 1260–1267.
- [177] Horka, M., Karasek, P., Roth, M., Ruzicka, F., *Anal. Bioanal. Chem.* 2018, *410*, 167–175.
- [178] Sun, J., Feng, J., Shi, L., Liu, L., He, H., Fan, Y., Hu, S., Liu, S., *J. Chromatogr. A* 2016, *1461*, 161–170.
- [179] Zhang, Y., Chen, W., Zhang, Y., Zhang, Y., Zhu, L., He, P., Wang, Q., *New J. Chem.* 2017, *41*, 12920–12929.
- [180] Xu, Z., Timerbaev, A. R., Hirokawa, T., *J. Chromatogr. A* 2009, *1216*, 660–670.
- [181] Xu, Z., Nakamura, K., Timerbaev, A. R., Hirokawa, T., *Anal. Chem.* 2011, *83*, 398–401.
- [182] Ye, X., Mori, S., Yamada, M., Inoue, J., Xu, Z., Hirokawa, T., *Electrophoresis* 2013, *34*, 583–589.
- [183] Burgi, D. S., Chien, R. L., *Anal. Biochem.* 1992, *202*, 306–309.
- [184] Burgi, D. S., Chien, R. L., *J. Microcolumn Sep.* 1991, *3*, 199–202.
- [185] Dawod, M., Breadmore, M. C., Guijt, R. M., Haddad, P. R., *J. Chromatogr. A* 2009, *1216*, 3380–3386.
- [186] Phung, S. C., Nai, Y. H., Macka, M., Powell, S. M., Guijt, R. M., Breadmore, M. C., *Anal. Bioanal. Chem.* 2015, *407*, 6995–7002.
- [187] Kwon, J. Y., Chang, S. B., Jang, Y. O., Dawod, M., Chung, D. S., *J. Sep. Sci.* 2013, *36*, 1973–1979.
- [188] Breadmore, M. C., Quirino, J. P., *Anal. Chem.* 2008, *80*, 6373–6381.
- [189] Breadmore, M. C., *Electrophoresis* 2008, *29*, 1082–1091.
- [190] Breadmore, M. C., *J. Chromatogr. A* 2010, *1217*, 3900–3906.
- [191] Lee, H. G., Kwon, J. Y., Chung, D. S., *Talanta* 2018, *181*, 366–372.
- [192] Dawod, M., Breadmore, M. C., Guijt, R. M., Haddad, P. R., *Electrophoresis* 2010, *31*, 1184–1193.
- [193] Abdul Karim, N., Wan Ibrahim, W. A., Sanagi, M. M., Abdul Keyon, A. S., *Electrophoresis* 2016, *37*, 2649–2656.
- [194] Thang, L. Y., Breadmore, M. C., See, H. H., *J. Chromatogr. A* 2016, *1461*, 185–191.

6 Addendum

²Department of Biopharmaceutics and Pharmacodynamics, Medical University of Gdansk, Gdansk, Poland

³ARC Centre of Excellence for Electromaterials Science (ACES), School of Natural Sciences, College of Science and Technology, University of Tasmania, Hobart, Australia

⁴Trajan Scientific and Medical, Ringwood, VIC, Australia

⁵Department of Chemistry, Lorestan University, Khoramabad, Iran

⁶Future Industries Institute (FII) University of South Australia, Mawson Lakes, Australia

⁷Department of Pharmaceutical Analytical Chemistry, Faculty of Pharmacy, Helwan University, Cairo, Egypt

⁸Department of Chemistry, Faculty of Science, Universiti Teknologi Malaysia, Johor Bahru, Johor, Malaysia

⁹Department of Pharmacy, Faculty of Pharmacy, Al-Zaytoonah University of Jordan, Amman, Jordan

¹⁰Centre for Sustainable Nanomaterials, Ibnu Sina Institute for Scientific and Industrial Research, Universiti Teknologi Malaysia, Johor Bahru, Johor, Malaysia

¹¹Centre for Personalized Nanomedicine, Australian Institute for Bioengineering and Nanotechnology (AIBN), The University of Queensland, Brisbane, QLD, Australia

¹²Department of Chemistry, University of Michigan, Ann Arbor, MI, USA